Mechanotransduction Pathways in Rigidity-sensitive and Rigidity-insensitive Cancer Cells

Catharine Randolph Cowan
Crozet, Virginia

B.A. Biology, University of Virginia, 2002

A Thesis presented to the Graduate Faculty
of the University of Virginia in Candidacy for the Degree of
Master of Science

Department of Microbiology

University of Virginia
August, 2010

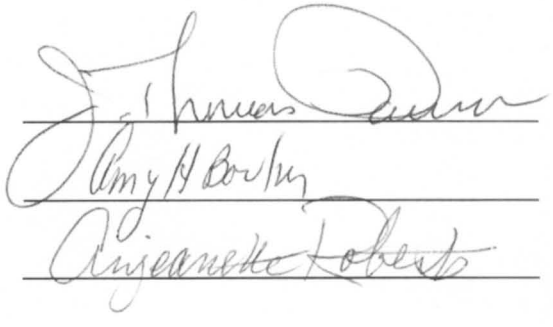

Acknowledgements

My journey towards this Master's thesis would never have progressed without the support of many people. First, thank you to the Microbiology department's academic advisory committee for allowing me to pursue this degree. It resulted in a lot of administrative wrangling on the part of Dr. AJ Roberts, Dr. Joel Hockensmith and Sandy Weirich, to whom I am greatly indebted. Thanks is also due to Drs. Amy Bouton and AJ Roberts for agreeing to be on my committee and read this thesis. None of this would have been possible if Dr. Tom Parsons had not had faith in my abilities and encouraged me to take the Molecular Basis of Carcinogenesis class. All of my labmates in the Parsons' lab have given me support whether through experimental suggestions, troubleshooting advice or simply offering a friendly ear when things weren't going well, I don't think I can bake enough cakes to thank them. Dr. Jill Slack-Davis has been both a dear friend and valuable "outside expert" for all things research related (and plenty that's not). Dr. Rob Tilghman, without whom this project wouldn't exist, has taught me not only how to be a good scientist, but how to be a good person in many ways. And finally, thank you to my husband, Brian. Without his love, support, patience and proofreading skills I would never have reached this point.

Abstract

Tissues and cells are subject to many physical forces, such as stress and strain. It has long been known that cells sense and respond to these physical forces. On a cellular level, the rigidity of surrounding extracellular matrix profoundly influences the physical forces sensed by normal cells and can inhibit or drive proliferation. Cancer cells, however, show varying growth responses to changes in rigidity. Comparison of multiple cell lines revealed that cancer cell growth responses generally fall into one of two categories: rigidity-sensitive or rigidity-insensitive. Cancer cells that are rigidity-insensitive grow efficiently regardless of their substrate rigidity, and likewise colonize soft tissue well. Rigidity-sensitive cancer cells proliferate more slowly on rigidities of soft tissue, but increase their growth dramatically as rigidity increases. These cells do not colonize soft tissue as well as rigidity-insensitive cells. To understand the mechanism by which cancer cells differ in their rigidity sensitivities, previously implicated mechano-sensory proteins were compared between four cell lines (two from each category). Comparison focused on three levels – that of transmembrane integrins, organization and dynamics of focal adhesions and organization of the actin/myosin cytoskeleton. While increased α_2-integrin levels correlated with rigidity-insensitivity, suppression of activity did not result in rigidity-specific responses, suggesting that integrins provide important growth signals but not in a mechano-sensitive way. In a screen of protein expression, p130Cas and myosin IIC were found to be over-expressed in the rigidity-insensitive cell lines. Interestingly, both proteins show a trend towards

decreased expression after growth on soft substrates for 5 days. Further work is required to understand the role these proteins play in rigidity responses. Finally, the myosin inhibitor blebbistatin was used to modulate tension in the cells and demonstrated the requirement for myosin activity in all the cell lines regardless of rigidity. Increased cell area in response to short-term blebbistatin treatment correlated with rigidity-insensitive cell lines. One possible explanation is that the rigidity-insensitive cells are under more tension than rigidity-sensitive cells on soft substrates. Taken together, these data indicate multiple levels of dysregulation that could promote growth in the rigidity-insensitive cancer cell lines, independent of extracellular physical cues.

Table of Contents

Tables and Figures

Abbreviations

ECM – extracellular matrix

FA – focal adhesion

MII – non-muscle myosin II heavy chain

IF – immunofluorescence

PA – polyacrylamide

TIRFM – total internal reflection fluorescence microscopy

Introduction

One of the most common ways solid tumors are identified is by palpation of a stiff lump within softer surrounding tissue. It is the physical properties, i.e. the stiffness, of the tumor and the surrounding microenvironment that enables discrimination from normal healthy tissue. Appreciation for the role that the physical properties of a tissue play in promoting cell growth and survival has emerged with the understanding of how cells sense their physical environment and transduce that information across signaling networks, a process referred to as mechanotransduction.

Physical forces and how they influence cellular homeostasis

The microenvironment for most tumors consists of other cells (myofibroblasts, inflammatory immune and vascular cells) and extracellular matrix (ECM) components such as collagen, laminin and fibronectin. The organization of these components significantly affects the rigidity that cells "feel" when attached to the matrix (Levental and others 2009). Both changes in deposition as well as crosslinking of ECM proteins can alter the matrix rigidity. Cells can "pull" on the ECM through adhesions and actin-associated motor proteins, thus generating tension within the cell along the adhesion-actin cytoskeleton connection. When the ECM is less rigid, the force the cell exerts will deform the surrounding matrix and less tension will be present in the cell. However, when the ECM is stiffer, an equal amount of force will not deform the matrix as much, resulting in the generation of more tension within the cell.

Tension causes aggregation of proteins into signaling complexes and can induce conformational changes that expose additional or novel binding sites in some proteins (del Rio and others 2009; Friedland, Lee, Boettiger 2009; Galbraith, Yamada, Sheetz 2002; Pelham and Wang 1997). These intracellular changes promote differential signaling and thus direct the cell's response to ECM rigidity.

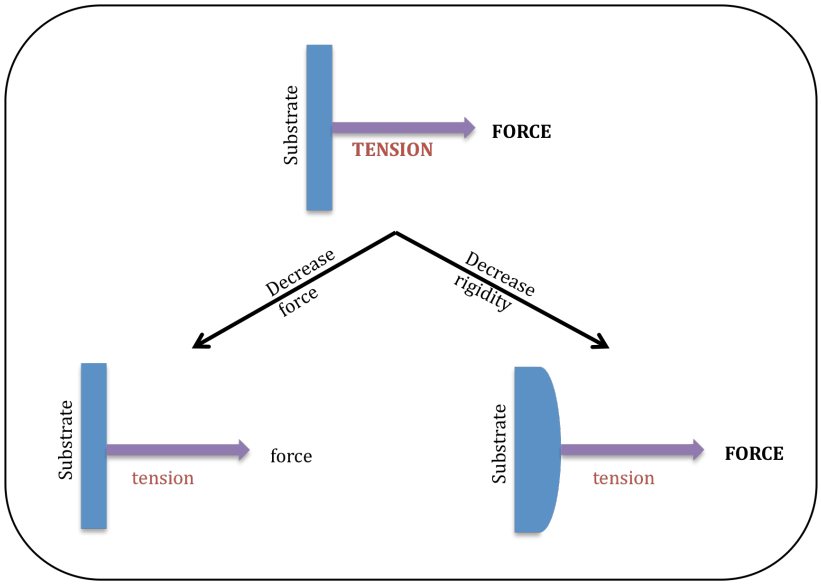

The relationship between tension and adhesion formation is cyclic. Integrin binding to ECM proteins forms an anchor on which focal adhesion proteins cluster, connect to actin, and then allow for tension generation by the action of myosin. Tension causes further clustering of integrins in the membrane, resulting in maturation of small, highly dynamic nascent adhesions to tension-dependent focal complexes and ultimately to mature focal adhesions (Choi and others 2008; Galbraith, Yamada, Sheetz 2002). The larger and more mature an adhesion, the more bundled actin and myosin are connected, and the greater the force that can be applied to the structure without disrupting protein interactions. Thus adhesion and tension perpetuate each other.

Tension generation in this context is dependent on the action of non-muscle myosin motors and this tension can be varied through regulation of myosin's activity. If myosin is inhibited, the cell cannot apply force to the ECM and tension is not generated within the cytoskeleton. Thus different levels of tension could be present within a cell due to modulation of myosin's activity. However, in fibroblasts the substrate rigidity and forces applied by the cell (measured by traction force microscopy) correlate linearly, suggesting tension generation is not uncoupled from ECM rigidity in non-tumorigenic cells (Paszek and others 2005). Myosin is regulated primarily through phosphorylation of the regulatory light chain subunit (MLC) (Vicente-Manzanares and others 2009). MLC can be phosphorylated by multiple kinases, including the Small GTPase-regulated Rho kinase (ROCK) (Somlyo and Somlyo 2003). While ROCK can directly phosphorylate MLC, it also phosphorylates the myosin phosphatase MYPT1, inactivating it and leading to buildup of phospho-MLC. MLC is also phosphorylated by myosin-light chain kinase (MLCK), which is regulated by calcium via interaction with calmodulin (Webb 2003).

Matrix rigidity regulates normal cell growth and drives cancer cell proliferation, migration, and survival

Rigidity and tension exert significant influence on cell growth, phenotype, and migration (Assoian and Klein 2008; Lo and others 2000; Paszek and others 2005; Wang, Dembo, Wang 2000). Mammary epithelial cells will form polarized, lumen-containing acini in compliant 3D collagen gels with little or no proliferation

(Wang and others 1998; Wozniak and others 2003). However, when embedded in stiff collagen, the cells form poorly organized clusters with more active proliferation and invasion into surrounding matrix (Paszek and others 2005). These cells respond to increasing rigidity with increased activation of the small GTPase Rho, Rho-dependent cellular tension, focal adhesion formation and focal adhesion kinase (FAK) activity, and elevated phosphorylation of the MAPK, ERK (Paszek and others 2005; Provenzano and others 2009). Klein et al. demonstrated rigidity growth responses are linked through another small GTPase, Rac, FAK activity and cyclin D expression, independent of ERK and Rho. The inconsistencies in the published data about Rho, Rac and ERK could be due to differences in cell type and culture conditions, but it is important to consider there might be multiple independent or cross-talking mechanotransduction signaling pathways that regulate growth according to rigidity of the ECM.

Normal cells respond to increasing rigidity with changes of behavior coined the “malignant phenotype”, including the loss of polarization and increased growth and invasiveness in collagen gels (Paszek and others 2005). Breast cancer cells display this same phenotype even when grown in collagen gels. While non-tumorigenic cells respond to changes in rigidity with changes in contractility, malignant cells demonstrate inherently greater contractility and higher Rho activity, and generate greater traction forces than non-malignant cell lines (Fritz, Just, Kaina 1999; Paszek and others 2005). Increasing rigidity has been shown to increase integrin expression in normal cells, while blockade of

integrins has been shown to suppress the abnormal phenotype of malignant cells (Wang and others 1998; Yeung and others 2005). The work done in the collagen gels suggests breast cancer cells have overcome at least some of the influence of the rigidity of the ECM and upregulate signals that would otherwise not be active in soft environments. In the context of metastatic disease, where a cancer cell must survive in suspension in the blood stream and colonize new sites in soft tissue, it would be necessary for the cancer cell to develop growth signaling independent of extracellular mechanical cues. However, how these cancer cells upregulate otherwise mechanically driven signals and whether this was a common phenomenon in all solid tumor types remains to be investigated.

Cancer cell growth responses to rigidity and mechanism

To address whether the malignant phenotype seen in soft gels was common to all tumorigenic cell lines, Dr. Robert Tilghman initiated a screen of cancer cell lines for growth responses to rigidity. The screen demonstrated the existence of two broad categories of responses: rigidity-sensitive and rigidity-insensitive. The patterns of rigidity sensitivity *in vitro* of four cell lines correlated with *in vivo* growth behavior in a soft environment, indicating the rigidity sensitivity of a particular cell line is an inherent property and not an artifact of artificial flexible substrates.

The primary goal of the work presented in this thesis is to understand how the rigidity-insensitive cancer cell lines have uncoupled signaling pathways that, in normal cells and rigidity-sensitive cancer cells, rely on mechanical cues. Two

rigidity-insensitive cell lines, mPanc96 and PC-3, and two rigidity-sensitive cell lines, MDA-MB-231 and A549, were used as models. It was hypothesized that altered proteins or signals critical for rigidity-insensitivity would occur somewhere within the pathways of mechanotransduction.

Analysis of the mechanotransduction machinery was approached from an outside-in strategy, targeting known mechano-sensitive modulators of growth. After a survey of known mutations in the cell lines failed to demonstrate correlation with rigidity sensitivity, collagen-binding integrin expression was evaluated in the different cell lines. Also, focal adhesion structure and protein expression were analyzed and the expression of myosin isoforms was compared. Finally, tension was manipulated in the cells with the myosin inhibitor blebbistatin to address whether the cells were dependent on myosin activity for growth on all rigidities, and what effect abolishing tension had on cell morphology on the different rigidity gels. These data offer preliminary insight into the altered mechano-sensory machinery present in cancer cells that may help overcome reliance on rigidity for proliferation.

Methods

Cell Lines and Antibodies

PC-3 and MDA-MB-231 cells were obtained from the MAPS Core at the University of Virginia. A549 were purchased from ATCC, and mPanc96 were a gift from Dr. Todd Bauer. PC-3, MDA-MB-231 and A549 were maintained in RPMI-1640 supplemented with 10% heat-inactivated fetal bovine serum (FBS) and penicillin/streptomycin at a concentration of 10units/10µg per mL. mPanc96 were maintained in DMEM supplemented with 10% FBS and 10units/10µg per mL penicillin/streptomycin.

The following flow cytometry antibodies were purchased from BD Biosciences: FITC anti-α_2-integrin, PE anti-α_1-integrin, APC anti-β_1-integrin, PE, FITC and APC anti-IgG1κ. Antibodies used for Western blotting and immunofluorescence were anti-paxillin (BD Biosciences), anti-FAK (Upstate), anti-ERK (a gift from Dr. Dan Gioeli), anti-Src (a gift from Dr. Sally Parsons), anti-p130Cas (a gift from Dr. Amy Bouton), anti-α_2-integrin (Millipore), anti-β-actin (Sigma), anti-myosin IIA and anti-myosin IIB (Covance), and anti-myosin IIC (Cell Signaling). Via-probe 7-AAD dye was purchased from BD Biosciences and Alexafluor 594-labeled phalloidin was purchased from Invitrogen/Molecular Probes.

Polyacrylamide substrates

The protocol for generation of polyacrylamide (PA) substrates was adapted from Wang and Pelham (Diagram 1) (Wang and Pelham 1998). Briefly,

solutions of acrylamide, bis-acrylamide, HEPES, ammonium persulfate and TEMED were applied to coverslips activated with 3-aminopropyltrimethoxysilane and glutaradehyde. The solution was overlaid with a silanized coverslip and allowed to polymerize. The resulting gels were activated in 6-well plates using the heterobifunctional crosslinker Sulfo-SANPANH and UV treatment, and then coated with 100ug/ml collagen I in PBS. The solutions used to generate the soft (150Pa) and stiff (4800Pa) gels are as follows: 3% acrylamide and 0.04% bis-acrylamide for the soft gels, and 7.5% acrylamide and 0.05% bis-acrylamide for stiff gels.

This protocol was adapted to glass-bottomed 96-well plates by Justin Mih and Dr. Dan Tschumperlin to generate the Softplate96, which they supplied for the growth experiments.

Growth assays

1000 cells were plated into each well of a Softplate96, such that seeding was in quadruplicate for each rigidity. Cells were cultured in 100-200µl of appropriate medium, with or without treatments. Cyquant NF cell proliferation assay from Invitrogen was used to quantify cell number at the end of 5 days. This kit uses a fluorescent DNA dye that is measured by a plate reader. A standard curve for each cell line was used to extrapolate actual cell number from fluorescence intensity.

In vivo lung colonization assay

Cancer cell lines were fluorescently labeled by infecting with a lentivirus encoding GFP. 1 x 10^6 cells in 200µl PBS were injected into the tail vein of 6-8 week-old nude mice (Taconic). Lungs were removed at 2-24 hours or 14 days following the injection and digested in collagenase (0.5 mg/ml in growth media) overnight at 37º C. Lung suspensions were homogenized by pipetting, and washed three times with PBS. The homogenates were fixed for 20 minutes at room temperature with 2% paraformldehyde in PBS, followed by washing twice with PBS and storage at 4º C for analysis by FACS. Samples were analyzed on a FACSCalibur Benchtop Analyzer and data acquired with Cell Quest software (Beckton Dickinson). 5x10^5 events were collected, and GFP positive cancer cells counted with FlowJo v.8.8.6. (Couresty of Dr. R. W. Tilghman)

Flow cytometry

Cells grown on collagen I coated plastic for 24hrs or on gel substrates for 5 days were scraped to dislodge and pipetted gently into suspension. 1x10^6 cells or less were centrifuged, resuspended in FACs staining buffer (2% FBS, 0.1% sodium azide, PBS) and blocked with 10µg non-specific mouse IgG for 10mins at room temperature. Antibodies and the viability dye Via-probe (7AAD) were added to this solution according to the manufacturer's recommendation and incubated for 45mins on ice. Cells were washed with 1ml of PBS, centrifuged, fixed in 2% paraformaldehyde (PFA) in PBS with 4µg/ml actinomycin D, and analyzed on a BD FACSCalibur within 24hrs. 10,000 raw events were acquired

for each sample. Using FlowJo v8.8.6, primary gates were drawn to exclude debris based on forward and side scatter. Singly stained controls were used to digitally compensate samples. Secondary gates were drawn around viable cells, i.e. those that excluded the viability dye. The viable populations were used to generate histograms of staining intensity. Isotype controls were used to bisect the histogram into negative and positive populations, such that 99% of the isotype peak was contained in the negative section. Counts of stained cells contained in the positive section were obtained.

Western Blotting and Densitometry

Cells were grown for 24hrs on collagen I coated plastic or for 5 days on gel substrates before being lysed in sample buffer (50mM Tris, 2% SDS, 10% glycerol, 0.1% bromophenol blue) with 8% β-mercaptoethanol. Lysates were subjected to standard SDS-Page electrophoresis then transferred to nitro-cellulose membranes. The membranes were blocked, probed with primary antibodies, then secondary HRP-labeled antibodies and detected by chemiluminescence. Multiple film exposures were obtained, and the best exposure deemed not to have saturated the film was used for densitometry. Films were scanned and the subsequent band intensities measured with the ImageJ densitometry plugin.

Immunofluorescence

Cells were grown on gels for 24hrs before being rinsed in PBS and fixed with 4% PFA in PBS. Coverslips were permeabilized with 0.5% Triton-X100 in PBS for 2mins, washed, then blocked in a solution of 20% goat serum and 5% BSA in PBS. Anti-paxillin was diluted 1:500 in block and incubated on the coverslips for 1hr. After washes, Alexafluor 488 anti-mouse and Alexafluor 594 phalloidin were diluted 1:500 in block and incubated on the coverslips for 1hr. Coverslips were mounted on slides and images collected with a Leica DMRBE microscope using a 60x oil objective and a Hammamatsu CCD camera operated by Openlab software. Image contrast and color were adjusted in Photoshop, and images were cropped and/or zoomed to highlight areas of interest.

Timelapse microscopy

Timelapse movies were acquired on a Nikon TE2000 microscope fitted with a Hammamatsu CCD camera at a magnification of 40x in DIC. Cells were maintained by a heated stage and overlay of mineral oil on the surface of the culture medium, as well as addition of 50mM HEPES. Images were taken at 3-second intervals for 3 minutes.

Statistics

ANOVA with Bonferroni's post-test was used to analyze lung colonization data. Paired T-test and Wilcoxon matched-pairs signed rank test was used to compare cell area before and after blebbistatin treatment.

Results

Growth responses to rigidity in four cancer cell lines

It has been demonstrated that cancer cells can grow in soft environments that do not support growth of normal cells (Huang and Ingber 2005). However, there has never been a comparison of rigidity growth response between cancer cells of different origin. Fourteen cell lines, encompassing prostate, breast, pancreatic and other cancers as well as fibroblasts and normal mammary epithelial cell lines were screened for their ability to grow on collagen-coated PA substrates ranging in rigidity from that observed in fatty soft tissue (150Pa) up to the rigidity of skeletal muscle (9600Pa) using the Softplate96 growth assay (Tilghman et al. manuscript submitted). While all of the cancer cell lines grew to some degree on the softest gels (data not shown), there were two main categories of growth responses: rigidity-sensitive and rigidity-insensitive (Fig. 1). Rigidity-sensitive cancer cell lines generate distinctive growth profiles characterized by little growth on the soft gels with incremental increase in fold growth as the rigidity increases, somewhat similar to non-tumorigenic cell lines. Rigidity-insensitive cell lines generate profiles of even proliferation regardless of the gel stiffness. The rigidity-sensitive cell lines are typified by the breast cancer line MDA-MB-231 and the non-small cell lung carcinoma line A549 (Fig. 1). Examples of rigidity-insensitive cell lines are the prostate cancer line PC-3 and the pancreatic cancer line mPanc96.

In vivo growth in soft tissue correlates with rigidity sensitivity

To determine if the distinction between rigidity-sensitive and rigidity-insensitive cells was an artifact of the Softplate96 format, four cancer cell lines were engineered to express GFP (mPanc96, PC-3, MDA-MB-231 and A549) and were injected into the tail vein of mice to colonize the lung. The rigidity of lung tissue averages 1200Pa (unpublished observation, Dr. D. Tschumperlin). Lungs were harvested after 4hrs and 14 days, the tissue digested with collagenase, and cells were sorted by flow cytometry to count GFP-positive cancer cells. The number of GFP-positive cells after 14days was compared to the number observed at 4hrs to account for variability in initial seeding (Tilghman et al. manuscript submitted). Comparison of the number of GFP-positive cells from both time points showed that the two rigidity-insensitive cell lines (mPanc96 and PC-3) proliferated significantly more than the rigidity-sensitive cell line, MDA-MB-231, and that the rigidity-sensitive A549 cells had a similar low rate of proliferation in soft lung tissue (Fig. 2A). In addition, lungs seeded with A549 or mPanc96 cells were collected over a 24hr time course to address concerns about differential clearing of cells from the lungs. There was no significant difference in cell number in the lungs after 24hrs.

Lungs from tumor cell injected mice were also collected for histological examination. 14 days after injection lung tissue was fixed and stained with hematoxylin and eosin to visualize tumor cell proliferation. The rigidity-sensitive cell lines did not form visible tumors while the rigidity-insensitive cell lines did (Fig. 2B). Taken together, these data demonstrate the growth response to

rigidity of each of these cell lines is an inherent property of the cell line, and not an artifact of culture conditions.

Mutation status of four cancer cell lines

Because some common mutations are known to promote proliferation in cancer cells, mutation data were collected for the four cancer cell lines previously characterized; PC-3, mPanc96, MDA-MB-231 and A549. The mutations in the mPanc96 cells were determined by PCR while the data for the PC-3, MDA-MB-213 and A549 were derived from the NCI-60 database. E-cadherin and N-cadherin expression was determined by Western blot. The mPanc96 cells had mutations in CDKN2A, K-Ras, and p53, and did not express either cadherin (Table 1). The PC-3 cells had mutations in p53 and PTEN, and expressed only N-cadherin. The MDA-MB-231 cells had mutations in BRAF, CDKN2A, K-Ras, and p53, and did not express either cadherin. The A549 cells had one mutation in K-Ras and did not express either cadherin when propagated on plastic. Previous work demonstrated upregulation of E-cadherin expression on soft gels after 5 days in the A549 cells (Tilghman et al. manuscript submitted). There was no obvious pattern of mutation that correlated with the rigidity-sensitive cell lines (MDA-MB-231 and A549) or rigidity-insensitive cell lines (mPanc96 and PC-3).

The role of collagen I binding integrins in rigidity sensitive growth of cancer cell lines

Integrins are responsible for bridging the gap between the interior of the cell and the ECM. Changes in conformation have long been known to play an important role in integrin activation and downstream signaling, and recently $\alpha_5\beta_1$ integrin has been shown to propagate focal adhesion signaling in a matrix rigidity-sensitive manner (Friedland, Lee, Boettiger 2009; Tzima and others 2001). The expression profiles of each subunit of the collagen I binding integrins ($\alpha_1\beta_1$ and $\alpha_2\beta_1$) were measured in the four different cancer cell lines. Staining with subunit specific antibodies and analysis by flow cytometry was used to measure surface expression of α_1-, α_2- and β_1- integrins in cells cultured on collagen-coated plastic. All cells expressed similar high levels of β_1-integrin, while α_1- and α_2-integrin expression varied (Fig. 3A). Approximately 50% of A549 and MDA-MB-231 and 60% of PC-3 were positive for α_1-integrin when compared to an isotype (negative) control; α_1 was not expressed on mPanc96 (Fig. 3B). α_2 expression by flow was higher in both rigidity-insensitive cell lines compared to rigidity-sensitive cells lines, correlating with the growth responses. The α_2-integrin surface expression was confirmed by Western blot with an α_2-specific antibody. Both the mPanc96 and PC-3 had higher total α_2 expression than the MDA-MB-231 and A549 (Fig. 4).

To determine if long-term growth on different rigidity gels might alter integrin expression levels, cells that had been cultured on either soft (150Pa) or stiff (4800Pa) gels for 5 days were stained for surface integrins as before and

analyzed by flow cytometry. The pattern of integrin expression after 5 days on the gels was similar to plastic and did not differ between soft and stiff gels (Fig. 5). The correlation between higher α_2 expression and rigidity-insensitive cell lines was conserved.

To test whether higher α_2 expression played a causative role in rigidity-insensitive growth, a 5 day growth assay was performed on the Softplate96 with a function-blocking α_2 antibody. Cells were either untreated, or grown in the presence of either 10μg/ml non-specific mouse IgG or 10μg/ml anti-α_2 integrin mAb. Growth of the PC-3 cells, which express both α_1-and α_2-subunits, was not affected by the α_2-blocking antibody (Fig. 6). However, mPanc96 cells showed significant decreases in growth on all rigidities due to treatment with the blocking antibody. These results indicate that while α_2-integrin plays an important role in providing a growth or survival signal on collagen I, it does not do so in a rigidity sensitive way.

Adhesion characteristics of cancer cell lines on different rigidity matrices

Focal adhesion (FA) formation stimulates multiple growth regulatory signaling pathways and also regulates cell protrusion and migration. Multiple proteins involved in FA formation have been implicated as mechano-sensors, including talin and p130Cas (del Rio and others 2009; Sawada and others 2006). Focal adhesion structure was compared on soft and stiff gels by immunofluorescence (IF) staining with anti-paxillin mAb to label adhesions and phalloidin to label the actin cytoskeleton. Actin stress fibers were present in PC-

3, MDA-MB-231 and A549 on the stiff gels (Fig. 7). The mPanc96 showed a bright cortical actin ring rather than stress fibers. Elongated paxillin-containing adhesions could be identified along some edges of all cells on the stiff gels. Cells on the soft gels were generally rounded and lacked stress fibers, however some of the cells had small protrusions. While punctate paxillin labeling could be seen in the cells on soft gels, it was not consistent or organized well enough to be clearly identified as focal adhesion staining, particularly using wide-field microscopy. Attempts were made to visualize adhesion structures by more sensitive methods, including total internal reflection fluorescent microscopy (TIRFM), however the optical properties of the PA gels make it impossible to reflect a laser on the surface of the gels (the critical component of TIRFM). Additionally confocal microscopy on both live cells with fluorescently tagged constructs as well as fixed and stained samples has not improved resolution of adhesion structures (data not shown).

Adhesion formation is necessary for stabilizing membrane protrusions, thus substrate-anchored protrusions are representative of adhesion formation. Since fluorescent methods were unsuccessful in identifying adhesions on soft gels, DIC movies of the cells on soft and stiff substrates were used to compare membrane protrusiveness in an indirect attempt to identify adhesion formation. The primary membrane activity of all the cell lines on the soft gels was blebbing (Fig. 8). The mPanc96 and A549 also demonstrated significant blebbing on the stiff gels as well. The PC-3 and MDA-MB-231 cells had lamellipodial-type protrusions on the stiff gels and significant membrane ruffling. Because of the

different phenotypes demonstrated on the different gels, kymograph quantification of membrane activity on soft versus stiff gels would not be informative. While the attempted protrusion analysis did not provide information about adhesion formation as hoped, it did demonstrate the blebbing phenotype that had not been observed previously.

Focal adhesion protein expression profiles

Amplification of protein expression is a common trait of cancer cells. It is possible that increased or decreased levels of some focal adhesion proteins might alter the stability of complexes or skew the signals generated. Additionally some FA proteins are mechano-sensitive, therefore expression levels of total ERK, FAK, Src and p130Cas were compared by Western blot between the rigidity-sensitive and rigidity-insensitive cell lines. Levels of ERK, FAK, and Src did not correlate with growth patterns, suggesting varying expression of these proteins does not contribute to rigidity-insensitive growth (Fig. 9). However, a trend of increasing p130Cas correlated with the rigidity-insensitive cell lines. Further testing is necessary to elucidate whether increased expression of p130Cas contributes to rigidity-insensitivity.

Myosin heavy chain expression profiles of cancer cell lines

Myosin motor proteins apply force across the actin cytoskeleton by cross-linking actin fibers anchored to FAs and mechanically sliding them against each other. The force applied generates tension, leading to clustering of molecules

and conformational changes that result in generation of pro-growth signals (Galbraith, Yamada, Sheetz 2002; Levental and others 2009). Since myosin-generated tension can lead to growth signals, the expression patterns of three myosin II heavy chain (MII) isoforms, MIIA, MIIB and MIIC, were compared between the four cell lines. Western blots were performed with isoform specific antibodies to probe for total protein expression. MHIIB expression was highest in MDA-MB-231 cell, similar in PC-3 and A549 cells and virtually undetectable in mPanc96 (Fig. 10). MIIA was expressed at roughly the same levels in all the cell lines. MIIC was expressed in mPanc96 and PC-3 to a greater degree than in A549, and poorly expressed (undetectable) in MDA-MB-231 cells. These data suggest that MIIA and MIIB protein expression levels do not play a role in rigidity-sensitivity, however there is a correlation between higher levels of MIIC and rigidity-insensitive growth that needs to be explored further.

Altered protein expression after culture on gels for 5days

Changes in matrix rigidity has been shown to regulate gene expression and protein levels (Engler and others 2006). Because the rigidity-sensitivity growth profiles were generated after 5 days of culture on the different rigidity gels, Western blots were done to compare expression of MIIC and p130Cas under the same conditions. The mPanc96 cells did not demonstrate any difference in expression of these proteins between the soft and stiff gels, however the other cell lines display a trend of decreasing expression on the soft gels after 5 days (except in the case of MDA-MB-231 cells which exhibited

undetectable levels of MHIIC) (Fig. 11). These observations indicate rigidity might also affect expression or stability of mechano-sensory proteins. However, it should be noted that the changes seen in p130Cas and MHIIC expression do not correlate with rigidity-sensitive growth.

Effects of myosin inhibition on growth and cellular morphology on different rigidity matrices

To assess the role of myosin in generating growth signals in the four different cancer cell lines on different rigidities, Softplate96 growth assays were performed with the addition of 10μM or 50μM blebbistatin, a pan-myosin II inhibitor. Treatment with 50μM blebbistatin abolished all growth, regardless of cell line or rigidity (Fig. 12). The 10μM treatment, which inhibits roughly 80% of the activity of MIIA *in vitro*, suppressed growth to varying degrees in all of the cell lines. While the overall fold growth was decreased, the rigidity-sensitive cells still responded to increasing rigidity with increased growth. The PC-3 cells maintained their rigidity-insensitive growth profile with 10μM blebbistatin treatment. The mPanc96 cells showed almost no change in growth with the 10μM blebbistatin on 1200Pa, 4800Pa and 19200Pa gels, while on the softest (300Pa) and stiffest (76800Pa) gels growth was suppressed. It is possible that because the mPanc96 cells grow only modestly on those rigidities (~4 fold) that incomplete suppression could be difficult to detect. However the experiment was performed only once in quadruplicate, therefore it should be repeated to confirm

the lack of effect of the 10μM blebbistatin treatment on the mPanc96 on moderate rigidities.

Blocking myosin activity with blebbistatin should reduce all myosin-driven tension. It has been demonstrated on glass that loss of tension results in disassembly of actin stress fibers as well as FAs (Liu and others 2010). To confirm this phenomenon also occurs on stiff gels, cells were grown on gels for 24hrs before treatment with 10μM blebbistatin for 24hrs. The cells on gels were then fixed and stained by IF for actin (red) and paxillin (green). The blebbistatin predictably eliminated actin stress-fiber formation and elongated FAs on the stiff gels in all of the cell lines (Fig. 13). There was no significant change in actin or paxillin staining on the soft gels with blebbistatin treatment, however it appeared the morphology of the PC-3 and MDA-MB-231 cells was altered dramatically.

To better visualize this change in morphology, images of cells on two different rigidities were acquired before and after 10μM blebbistatin treatment. While there was not a dramatic change in cell size or shape at 1hr, by 24 hrs the MDA-MB-231 and PC-3 cells had elongated significantly on the soft gels, such that their morphology with blebbistatin treatment on soft and stiff gels were very similar (Fig. 14). The mPanc96 cells maintained a rounded shape regardless of rigidity or blebbistatin treatment. The A549 cells were rounded on the soft gel and more spread on the stiff gel both before and after blebbistatin treatment. Previous work demonstrated that the rigidity-sensitive cell lines had a significant difference in cell morphology on different rigidities while the rigidity-insensitive

cell lines had little to no change of morphology (Tilghman et al., manuscript submitted). That correlation is abolished with blebbistatin treatment.

Cells have a basal level of myosin activity that presumably keeps the cell under a basal level of tension. Blebbistatin treatment should rapidly release that basal tension. The low-resolution phase images did not show a significant change in cell morphology at 1 hr, however subtle changes would have been hard to detect. Therefore higher resolution DIC movies of cells on soft and stiff gels treated with 10μM blebbistatin were acquired. A change in cell area was observed on the soft gels in the PC-3 and mPanc96 cells, and a more significant retraction response was noted on stiff gels in all the cell lines (data not shown). To quantify these changes, cell areas were measured (in pixels) before treatment and 30mins after. The 30 min area was subtracted from the initial area to generate a Δ area (ΔA) value for each cell. Positive values indicate an increase in cell area with treatment while negative values indicate a decrease in cell area. The measurements agreed with the initial observations, that all the cell lines showed a significant decrease in cell area compared to their initial areas on the stiff gels (Fig. 15). On the soft gels, the A549 and MDA-MB-231 cells showed almost no change with blebbistatin treatment while the PC-3 cells increased significantly in size, and the mPanc96 had a similar trend. While tension reduction with blebbistatin treatment results in contraction of cells on stiff gels in all the cell lines, on the soft gels there was an increase in cell area only in the rigidity-insensitive cell lines. The increase in cell area could be due to release of tension stored in the gel substrate and cytoskeleton, or could be due to actin

polymerization. The experimental design did not allow for discrimination of the source driving the increase in cell area of the PC-3 and mPanc96.

Figures

Diagram 1: **Polyacrylamide gel substrate systems.** A) Outline of procedure for generation of 2D gel substrates used for biochemical experiments and microscopy. B) Illustration of Softplate96 substrate rigidity gradient.

Diagram 1

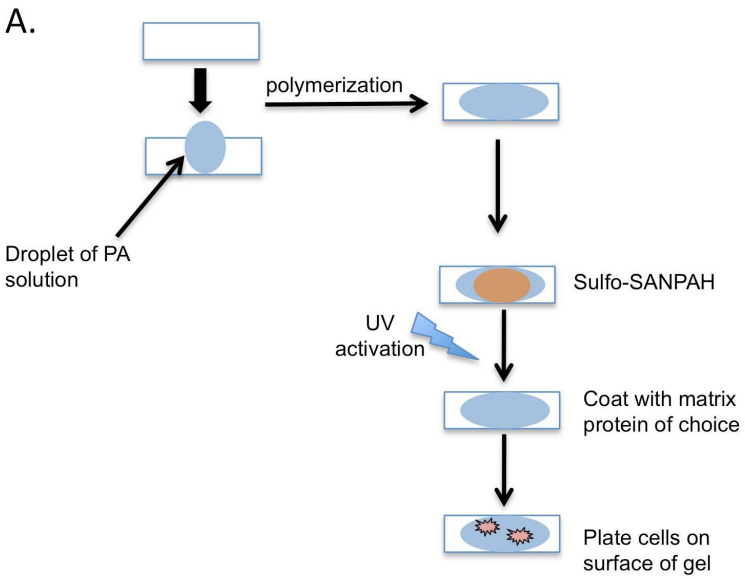
A.
polymerization
Droplet of PA solution
Sulfo-SANPAH
UV activation
Coat with matrix protein of choice
Plate cells on surface of gel

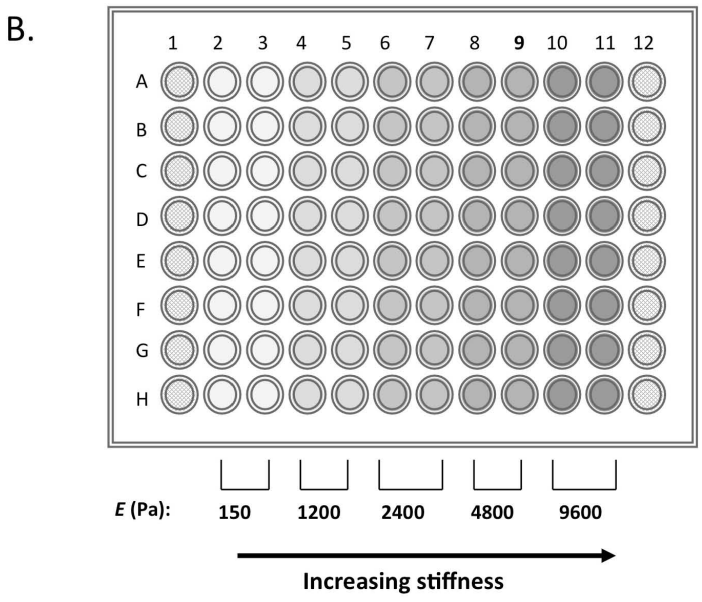
B.
1 2 3 4 5 6 7 8 9 10 11 12
A
B
C
D
E
F
G
H
E (Pa):
150
1200
2400
4800
9600
Increasing stiffness

Figure 1: **Growth profiles of rigidity-sensitive and rigidity-insensitive cell lines.** Graphs represent fold growth after 5 days on the Softplate96, measured by Cyquant assay.

Figure 1

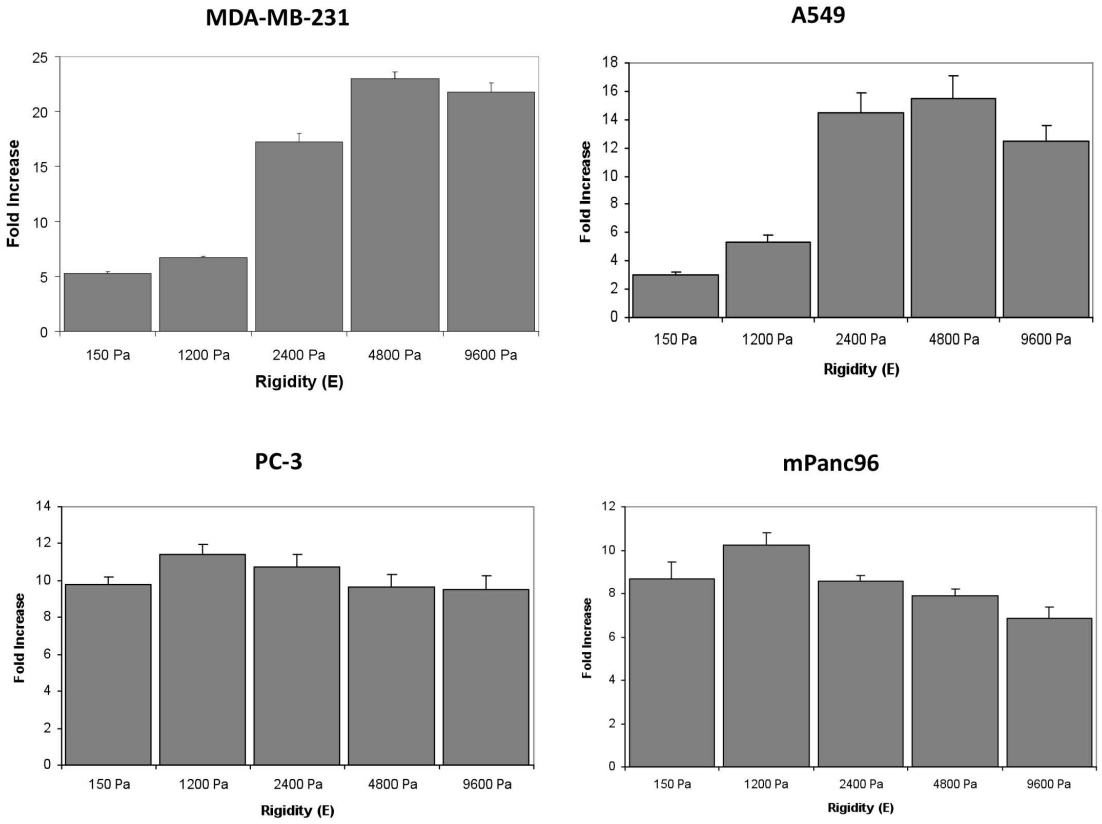

Courtesy of R. Tilghman

Figure 2: **Growth of cancer cell lines in mouse lung**. A) GFP-expressing cancer cell lines (mPanc96, PC-3, MDA-MB-231 and A549) were seeded in the lungs of nude mice by tail vein injection. Cells present in the lungs, as measured by flow cytometry, are expressed as the fold increase in cell number after 14days from a 4hr initial count. Inset graph represents cell counts over a 24hr time-course after injection of either A549 or mPanc96 cells. B) Histology of lung samples after 14 days of injection with either A549 (left panel) or mPanc96 cells (right panel). Arrows indicate micro-metastases.

Figure 2

A.

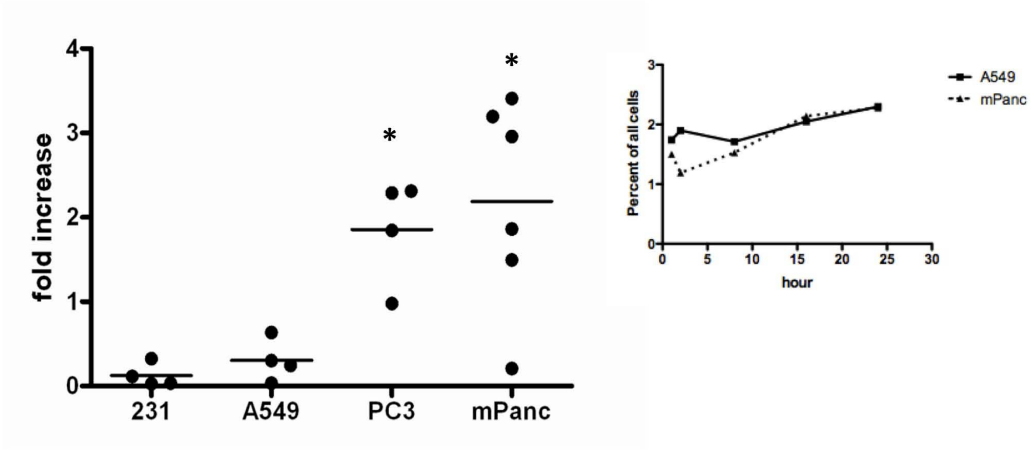

*p<0.05

B.

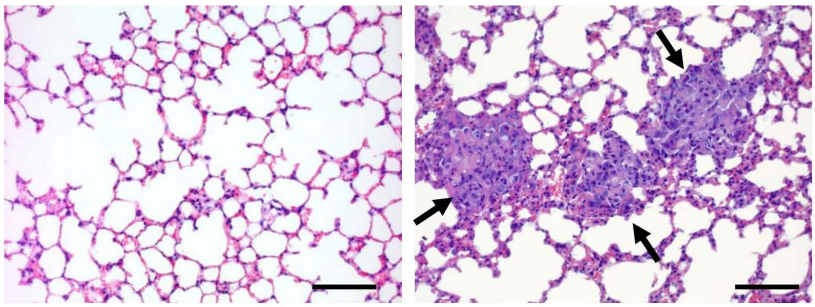

Courtesy of R. Tilghman

Table 1: **Known mutations in four cancer cell lines.** Mutation data for four cancer cell lines, two rigidity-sensitive (MDA-MB-231 and A549) and two rigidity-insensitive (mPanc96 and PC-3). Data for the PC-3, MDA-MB-231 and A549 was derived from the NCI-60 cell line database. mPanc96 mutations were determined by PCR, and the cadherin expression was evaluated by Western blot.

Table 1

		Cell Line		
Protein	**mPanc96**	**PC-3**	**MDA-MB-231**	**A549**
BRAF	WT	WT	mutant	WT
CDKN2A	mutant	WT	mutant	WT
EGFR		WT	WT	WT
FAK				
K-Ras	mutant	WT	mutant	mutant
Myc		WT	WT	WT
NF 1		WT	WT	WT
NF 2		WT	mutant	WT
Nras		WT	WT	WT
p53	mutant	mutant	mutant	WT
PDGFR		WT	WT	WT
PTEN		mutant	WT	WT
RB1		WT	WT	WT
SMAD4	WT	WT	WT	WT
E-cadherin	neg		neg	?
N-cadherin	neg	pos	neg	neg

Figure 3: **Collagen I binding integrin profile of four cancer cell lines.** A) Representative histograms of integrin surface expression as determined by flow cytometry. B) Percent of cells positively expressing each integrin. Cells with staining intensity above an isotype negative gate were considered positive and counted. Counts are expressed as percentages of all viable cells. Graph represents the average of two experiments ± SEM. 10,000 events were counted for each sample.

Figure 3

A.

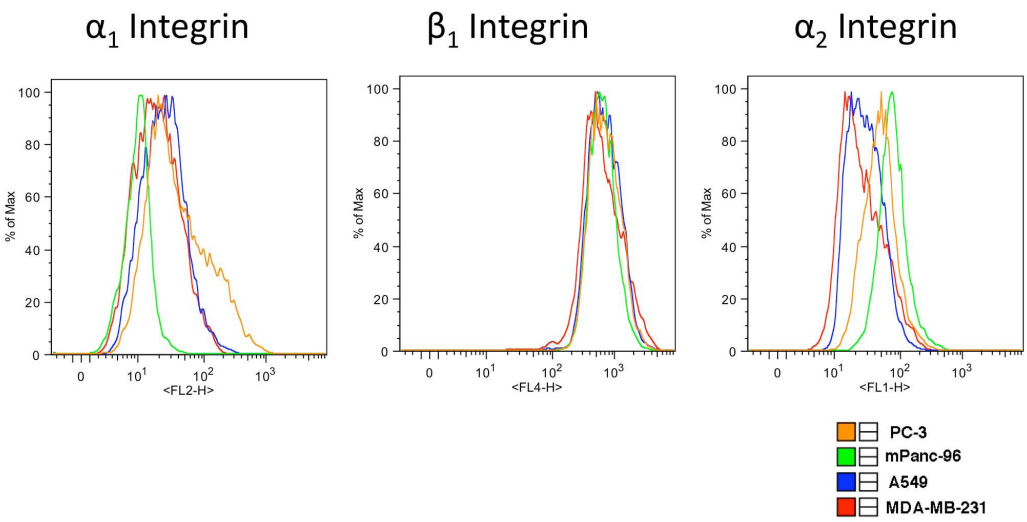
α1 Integrin
β1 Integrin
α2 Integrin
% of Max
<FL2-H>
<FL4-H>
<FL1-H>
PC-3
mPanc-96
A549
MDA-MB-231

B.

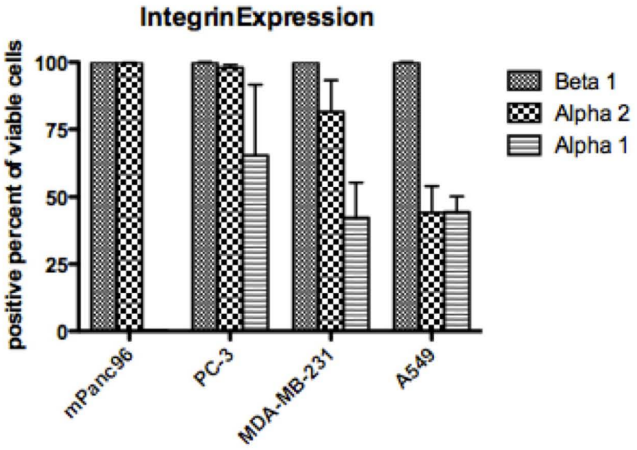
IntegrinExpression
positive percent of viable cells
Beta 1
Alpha 2
Alpha 1
mPanc96
PC-3
MDA-MB-231
A549

Figure 4: **Total protein expression levels of α_2-integrin.** Representative Western blot of α_2-integrin in the four cancer cell lines. The graph represents densitometry performed on two independent experiments where α_2 was normalized to β-actin levels. Error bars are $\pm$ SEM.

Figure 4

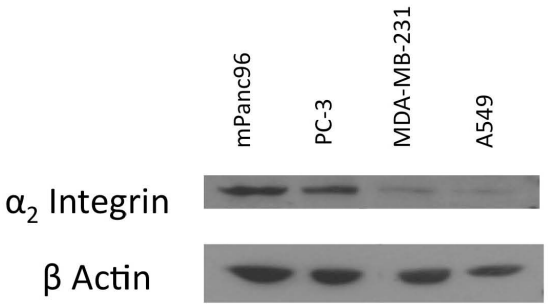
mPanc96
PC-3
MDA-MB-231
A549
α2 Integrin
β Actin

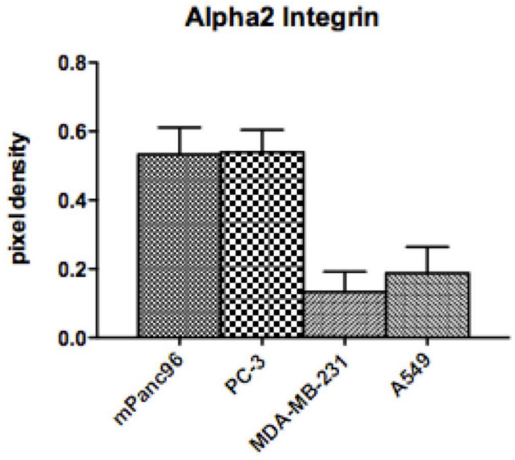
Alpha2 Integrin
pixel density
0.8
0.6
0.4
0.2
0.0
mPanc96
PC-3
MDA-MB-231
A549

Figure 5: **Expression of integrins on different rigidity substrates.** Cells were plated on soft (150Pa) or stiff (4800Pa) PA gels for 5 days. The cells were scraped off the gels and stained for analysis by flow cytometry. The red line represents cells from the soft gels; the blue line represents cells from the stiff gels. 10,000 events were counted for each graph.

Figure 5

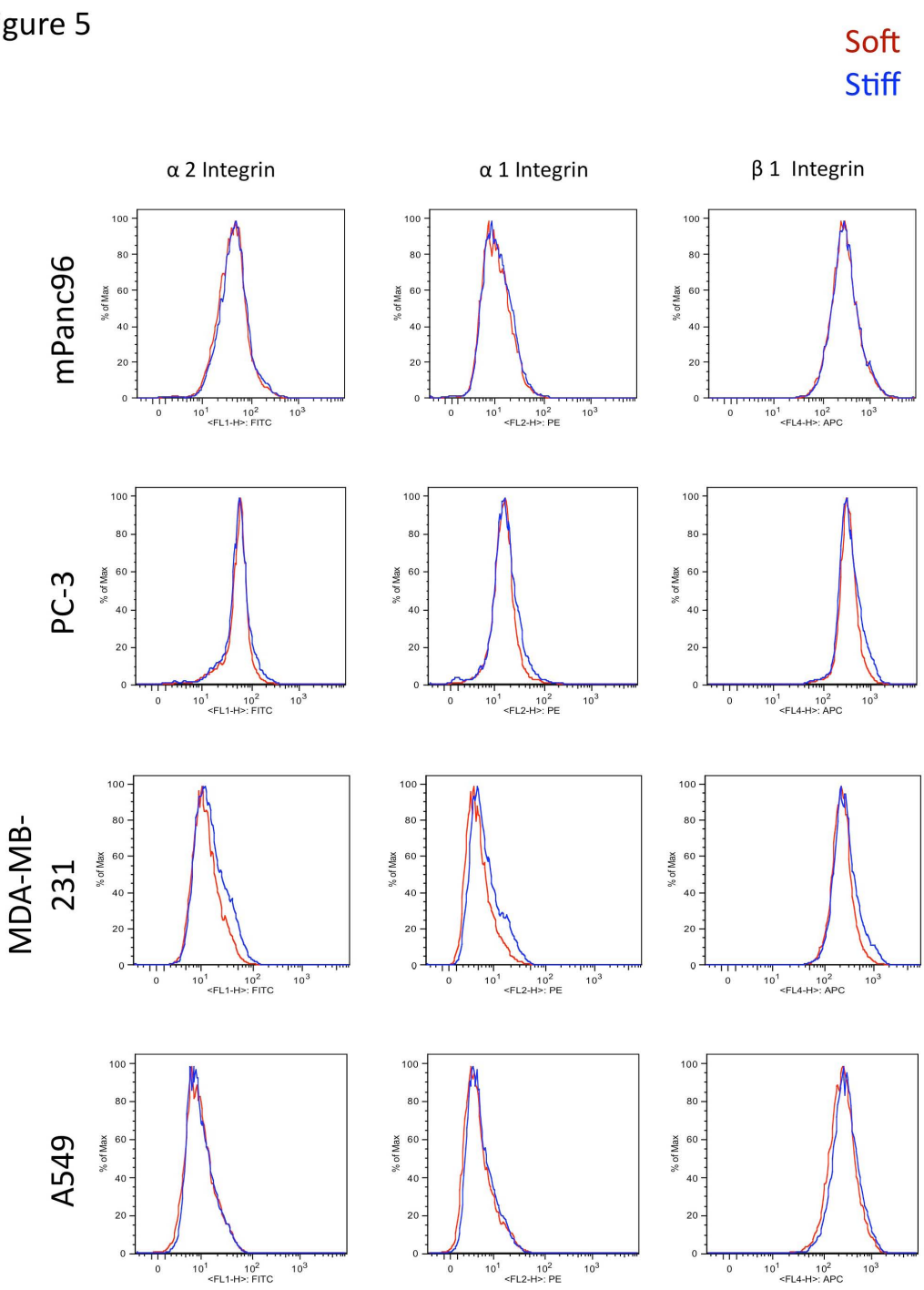
Soft
Stiff
α 2 Integrin
α 1 Integrin
β 1 Integrin
mPanc96
PC-3
MDA-MB-231
A549
% of Max
<FL1-H>: FITC
<FL2-H>: PE
<FL4-H>: APC

Figure 6: **Growth patterns of rigidity-insensitive cell lines with an α_2-integrin blocking antibody.** A 5 day Softplate96 growth assay was performed with 10μg/ml of either mouse IgG or a function blocking α_2 antibody, or no treatment. The graph represents the average of one experiment in quadruplicate, $\pm$ SEM.

Figure 6

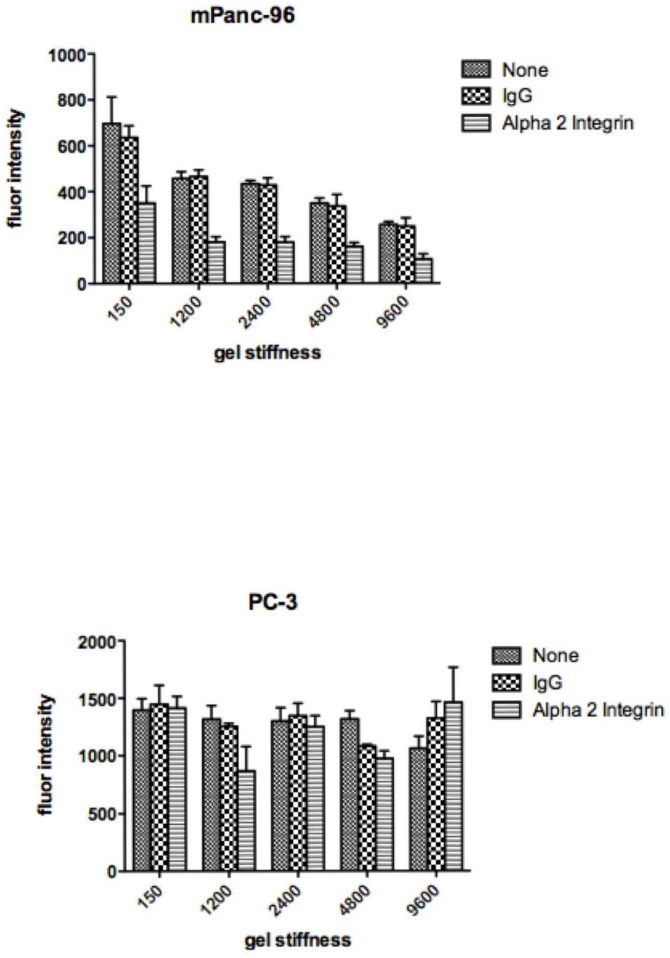
mPanc-96
fluor intensity
1000
800
600
400
200
0
150
1200
2400
4800
9600
gel stiffness
None
IgG
Alpha 2 Integrin
PC-3
fluor intensity
2000
1500
1000
500
0
150
1200
2400
4800
9600
gel stiffness
None
IgG
Alpha 2 Integrin

Figure 7: **Cytoskeletal and adhesion morphology on different rigidity substrates.** Immunofluorescence staining for actin (red) and paxillin (green) of each cell line on soft or stiff gels. Paxillin images include a zoomed quadrant for visualization of focal adhesion detail.

Figure 7

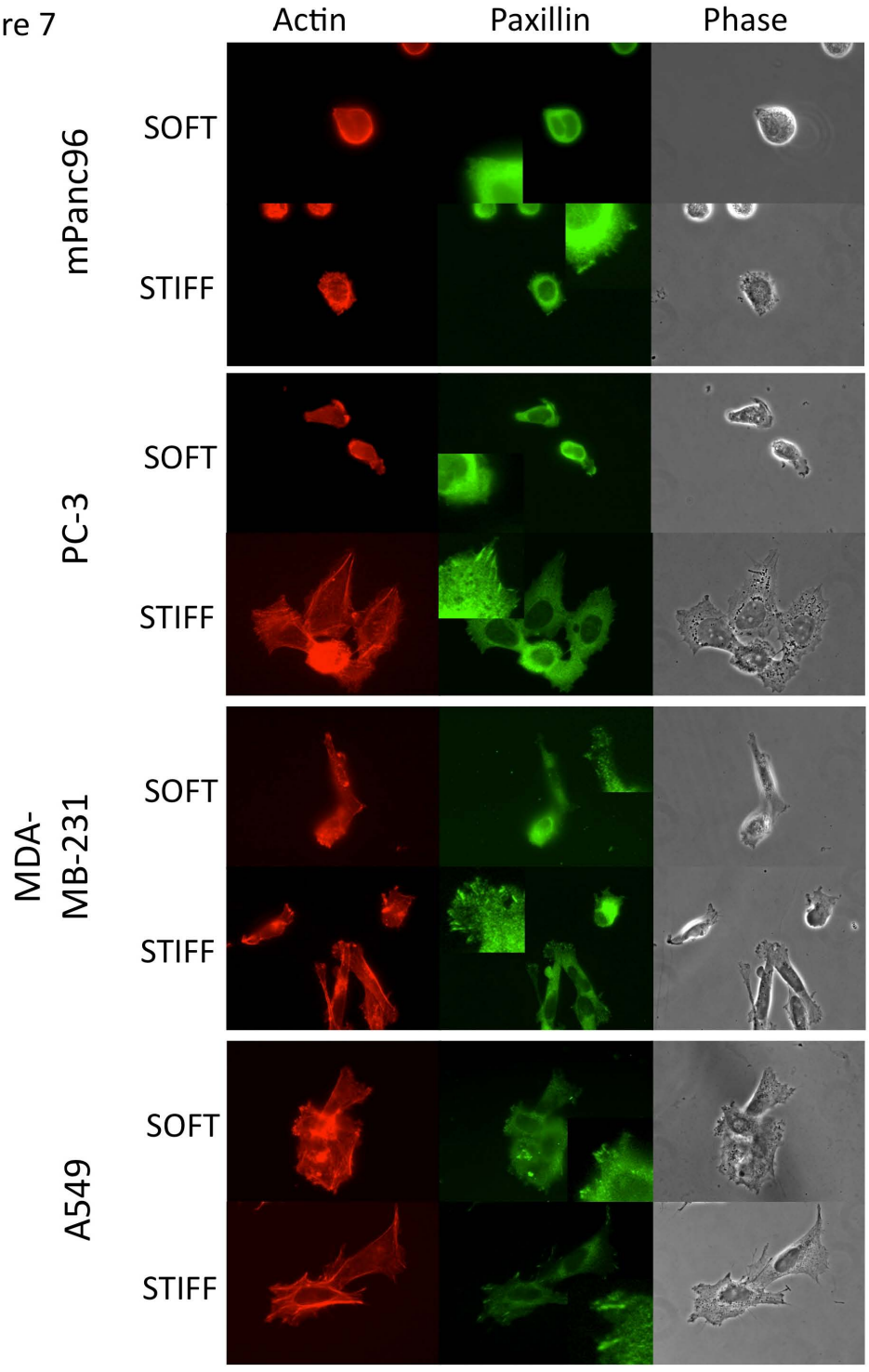
Actin
Paxillin
Phase
mPanc96
SOFT
STIFF
PC-3
SOFT
STIFF
MDA-MB-231
SOFT
STIFF
A549
SOFT
STIFF

Figure 8: **Cell membrane morphology on different rigidity substrates.** Each cell line was plated on soft gels, stiff gels or collagen-coated glass for 24hrs before being imaged by DIC. Each image is the first frame of a 3-minute timelapse movie.

Figure 8

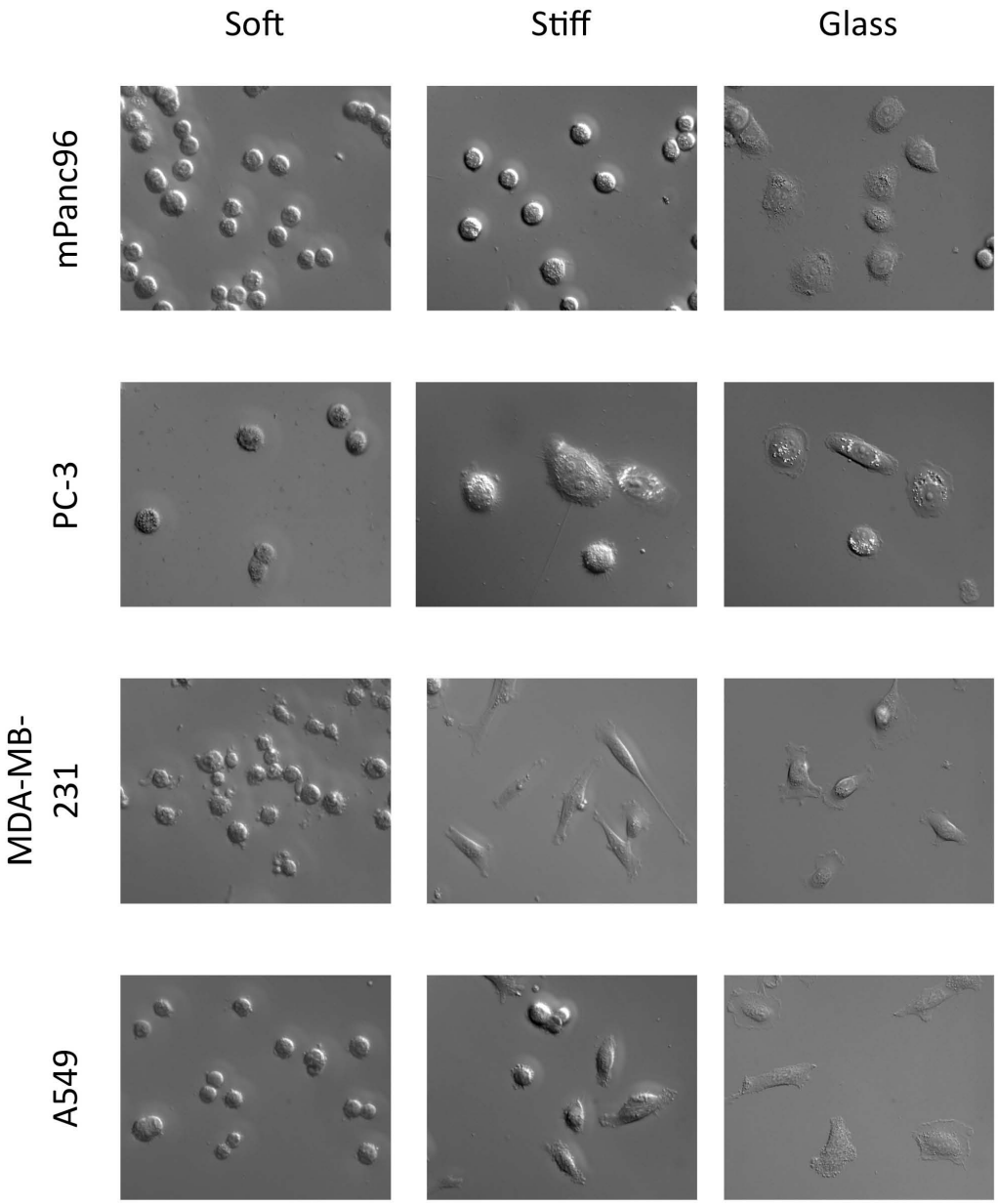

Figure 9: **Adhesion and signaling protein expression in the four cancer cell lines.** Lysates of the four cell lines collected from plastic were subjected to Western blotting with ERK, FAK, Src, p130Cas and β-actin specific antibodies. The graphs represent densitometry analysis where the individual protein levels were normalized to β-actin. The ERK and Src graphs are the average of three and two experiments respectively, ± SEM, while the FAK and p130Cas are from one experiment.

Figure 9

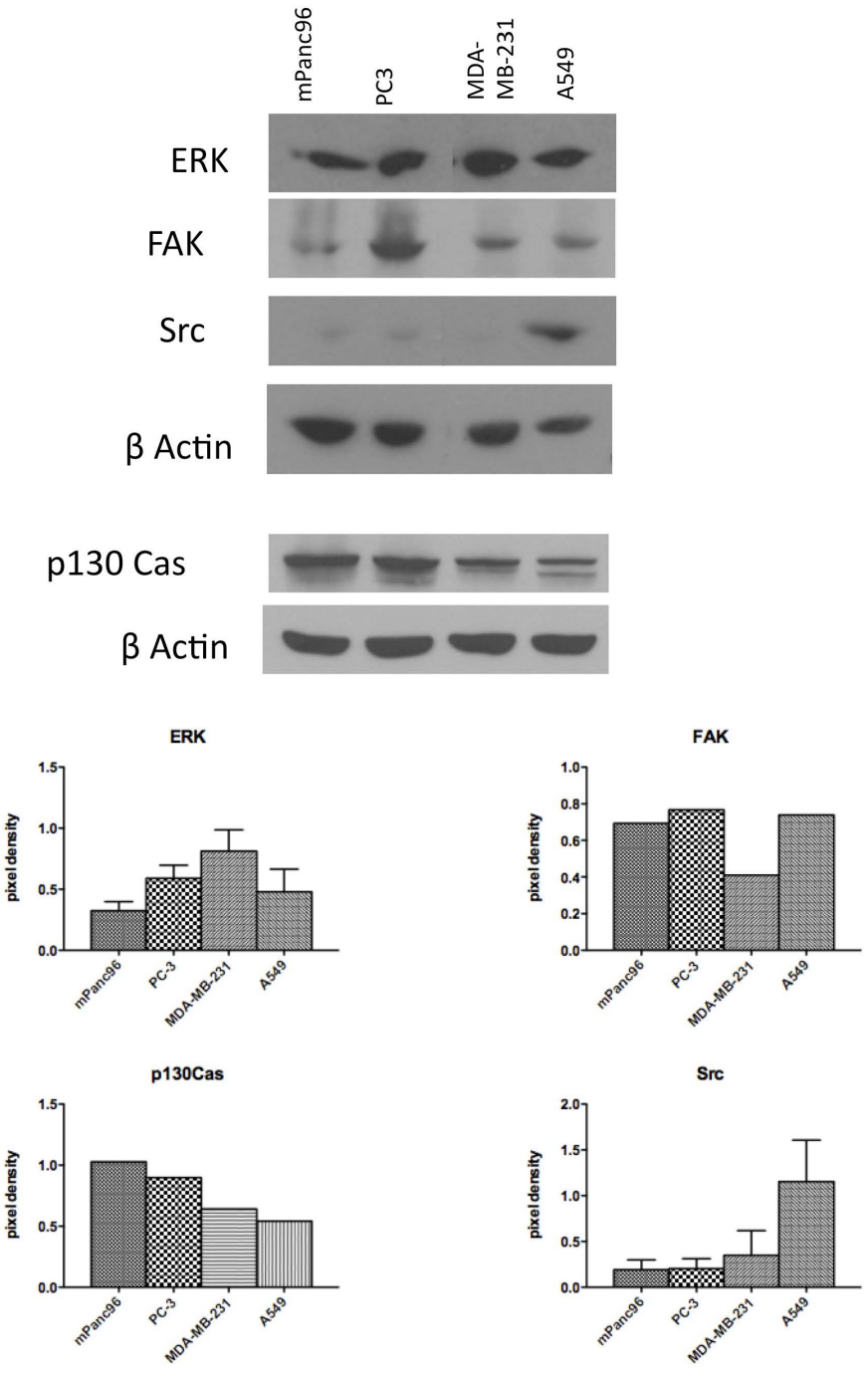
mPanc96
PC3
MDA-MB-231
A549
ERK
FAK
Src
β Actin
p130 Cas
β Actin
ERK
FAK
p130Cas
Src
pixel density
mPanc96
PC-3
MDA-MB-231
A549

Figure 10: **Expression of different myosin II heavy chain isoforms in the four cancer cell lines.** Western blots for MHIIA, MHIIB and MHIIC were performed on lysates from cells grown on plastic. The graphs represent densitometry analysis where myosin heavy chain protein levels were normalized to β-actin. Densitometry data for MHIIB and MHIIA are the average of two experiments ± SEM. Densitometry data for MHIIC are from one experiment.

Figure 10

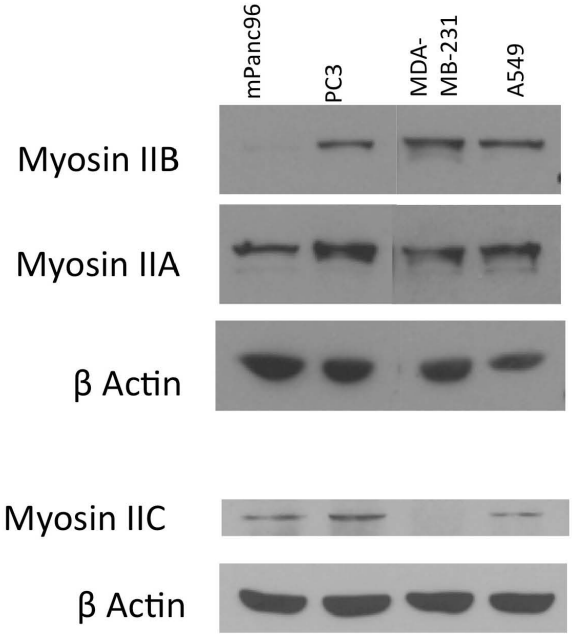
mPanc96
PC3
MDA-MB-231
A549
Myosin IIB
Myosin IIA
β Actin
Myosin IIC
β Actin

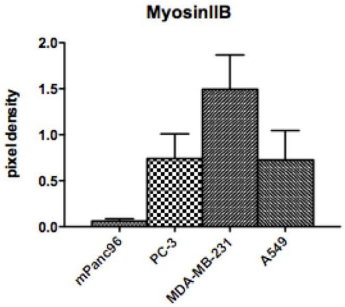
MyosinIIB
pixel density
2.0
1.5
1.0
0.5
0.0
mPanc96
PC-3
MDA-MB-231
A549

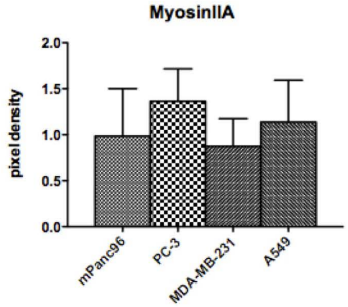
MyosinIIA
pixel density
2.0
1.5
1.0
0.5
0.0
mPanc96
PC-3
MDA-MB-231
A549

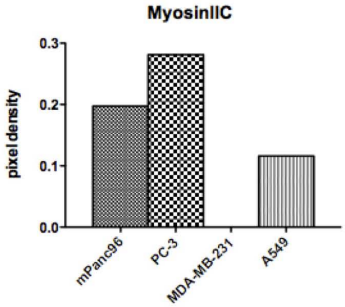
MyosinIIC
pixel density
0.3
0.2
0.1
0.0
mPanc96
PC-3
MDA-MB-231
A549

Figure 11: **Protein expression patterns after 5 day culture on different rigidities.** Western blots on lysates from cells grown on either soft or stiff gels for 5 days. The graphs represent densitometry quantification where the levels of each protein were normalized to β-actin. Graphs are the average of two experiments, ± SEM.

Figure 11

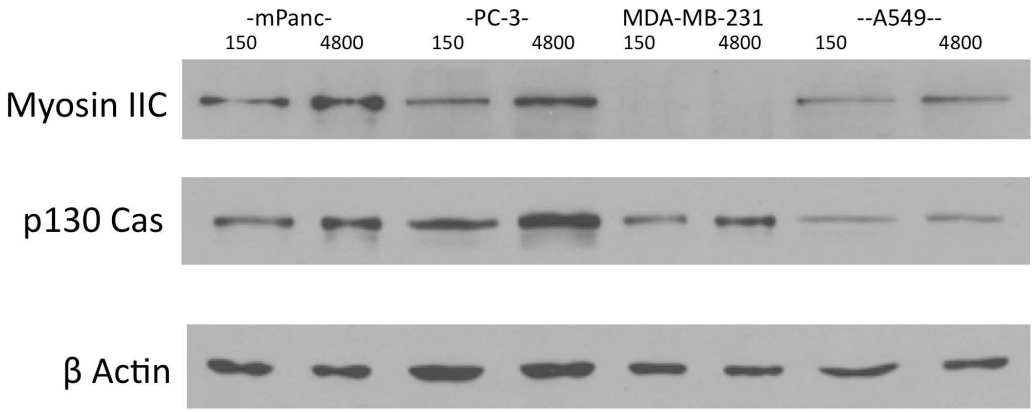
-mPanc-
-PC-3-
MDA-MB-231
--A549--
150
4800
150
4800
150
4800
150
4800
Myosin IIC
p130 Cas
β Actin

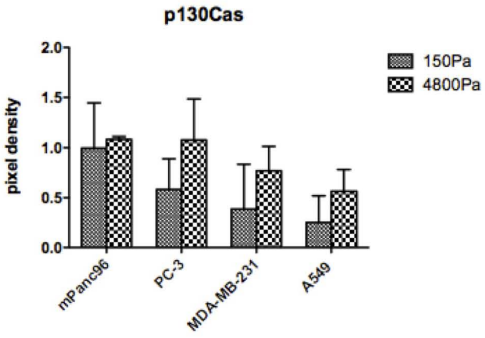
p130Cas
pixel density
2.0
1.5
1.0
0.5
0.0
150Pa
4800Pa
mPanc96
PC-3
MDA-MB-231
A549

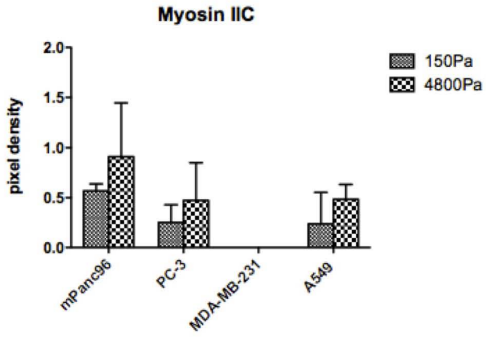
Myosin IIC
pixel density
2.0
1.5
1.0
0.5
0.0
150Pa
4800Pa
mPanc96
PC-3
MDA-MB-231
A549

Figure 12: **Effects of blebbistatin on growth on different rigidities.** A 5 day Softplate96 growth assay was performed with 10μM or 50μM blebbistatin treatment, or DMSO control. Each graph represents the average of one experiment in quadruplicate, ± SEM.

Figure 12

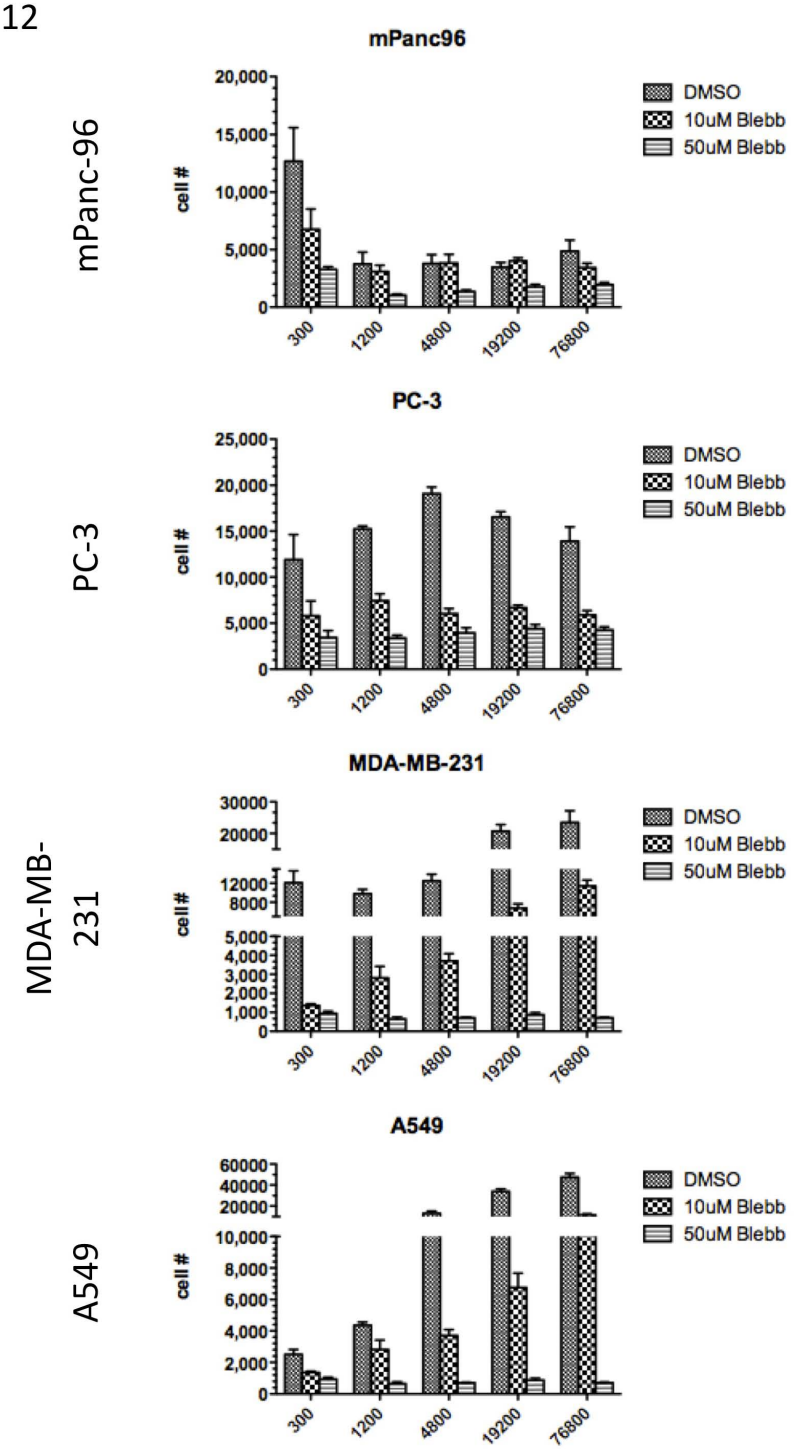
mPanc96
mPanc-96
cell #
20,000
15,000
10,000
5,000
0
300
1200
4800
19200
76800
DMSO
10uM Blebb
50uM Blebb
PC-3
PC-3
cell #
25,000
20,000
15,000
10,000
5,000
0
300
1200
4800
19200
76800
DMSO
10uM Blebb
50uM Blebb
MDA-MB-231
MDA-MB-231
cell #
30000
20000
12000
8000
5,000
4,000
3,000
2,000
1,000
0
300
1200
4800
19200
76800
DMSO
10uM Blebb
50uM Blebb
A549
A549
cell #
60000
40000
20000
10,000
8,000
6,000
4,000
2,000
0
300
1200
4800
19200
76800
DMSO
10uM Blebb
50uM Blebb

Figure 13: **Effects of blebbistatin on adhesion and cytoskeletal morphology on different rigidities.** Immunofluorescence staining (IF) for actin (red) and paxillin (green) of cells on gels with and without blebbistatin treatment. Cells were plated on soft and stiff gels for 24hrs, and then treated with 10μM blebbistatin for another 24hrs before fixation and IF.

Figure 13

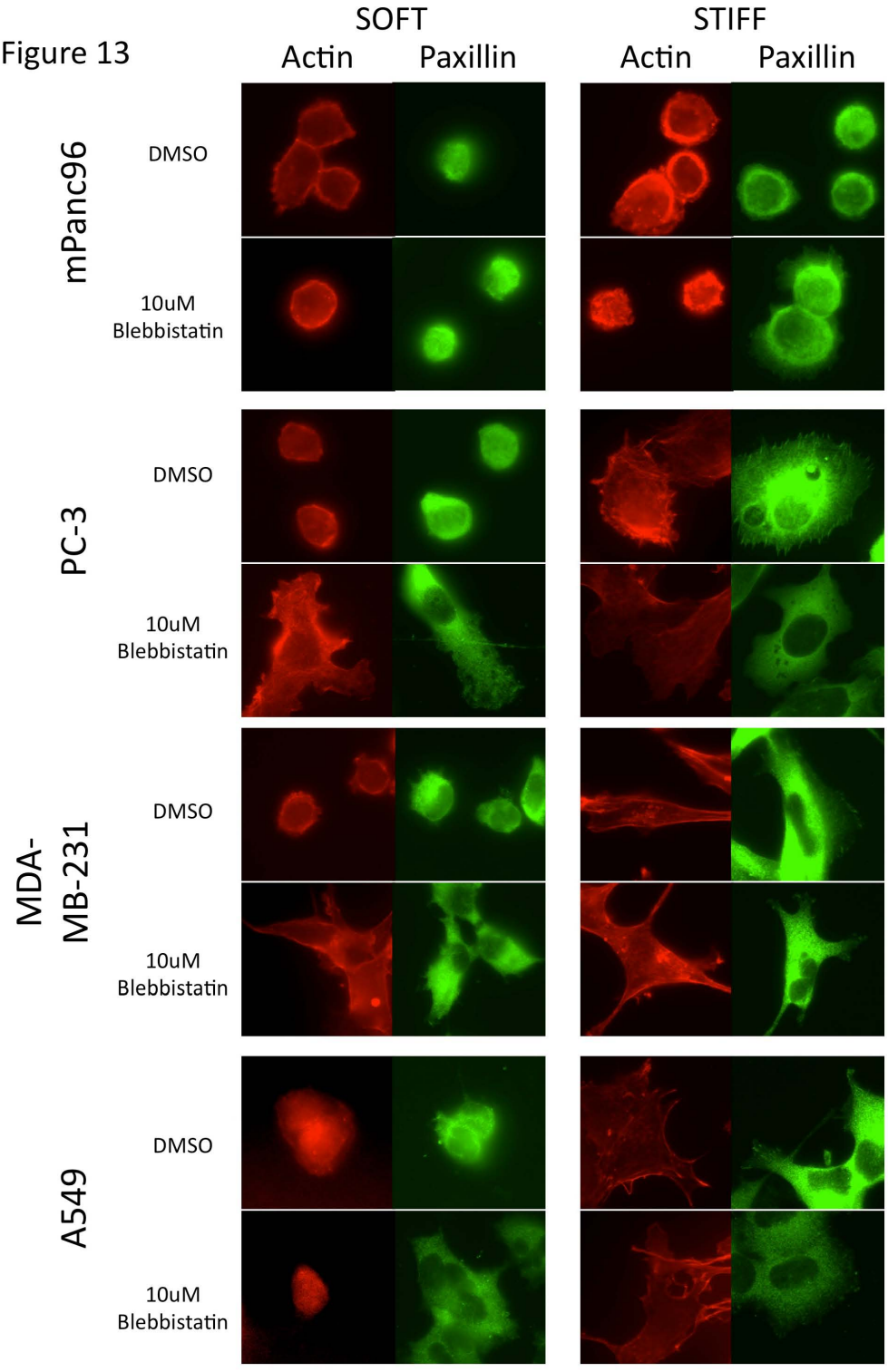
SOFT
STIFF
Actin
Paxillin
Actin
Paxillin
mPanc96
DMSO
10uM Blebbistatin
PC-3
DMSO
10uM Blebbistatin
MDA-MB-231
DMSO
10uM Blebbistatin
A549
DMSO
10uM Blebbistatin

Figure 14: **Effects of blebbistatin on cell morphology on different rigidities.** Phase contrast images of the cells were acquired immediately before addition of 10μM blebbistatin and at 1hr and 24hrs post treatment.

Figure 14

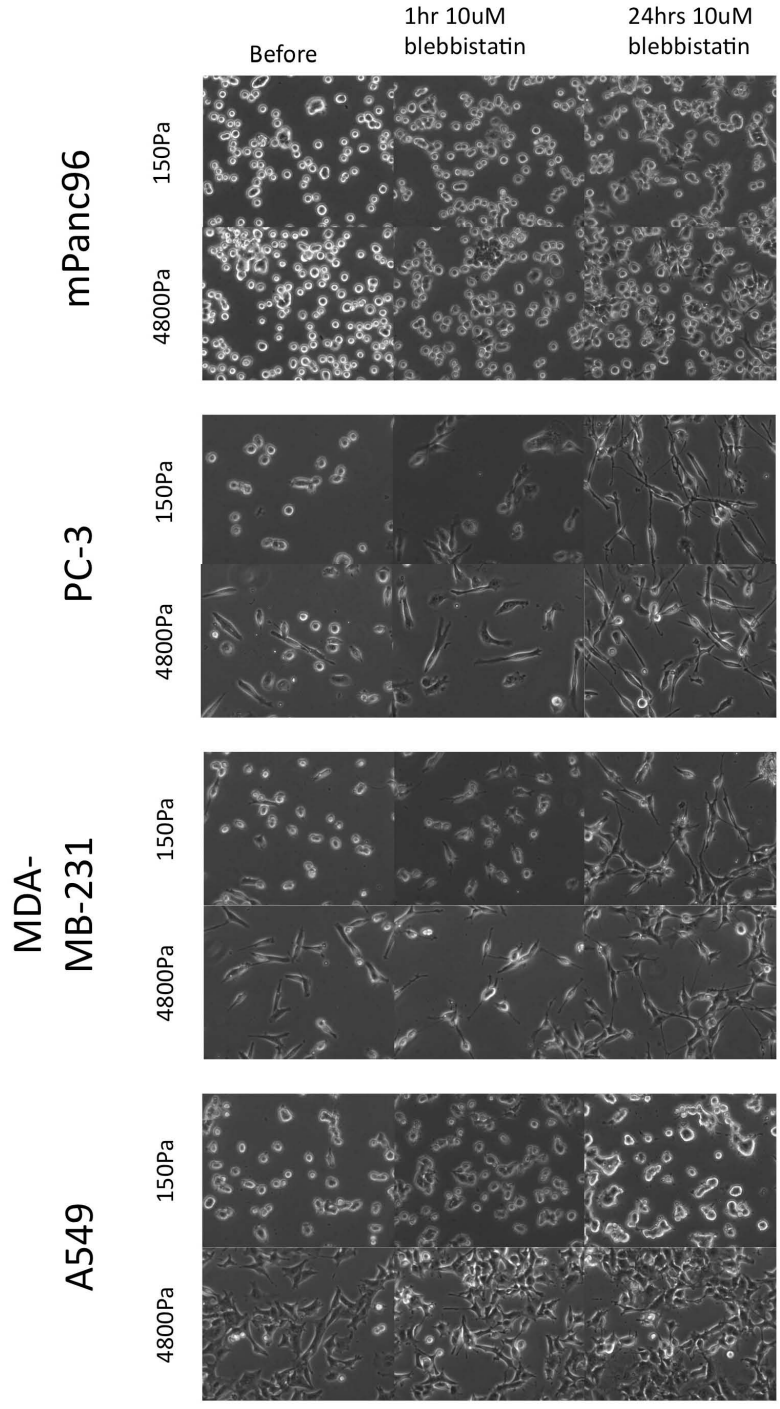
Before
1hr 10uM blebbistatin
24hrs 10uM blebbistatin
mPanc96
PC-3
MDA-MB-231
A549
150Pa
4800Pa

Figure 15: **Short-term blebbistatin-induced changes in cell area.** Graphs represent changes in cell area due to blebbistatin treatment. DIC images of cells immediately before 10μM blebbistatin addition and 30mins after were used to measure cell area. The area after addition, measured in pixels, was subtracted from the initial area to obtain a positive or negative ΔA. Each point represents the ΔA of one cell.

Figure 15

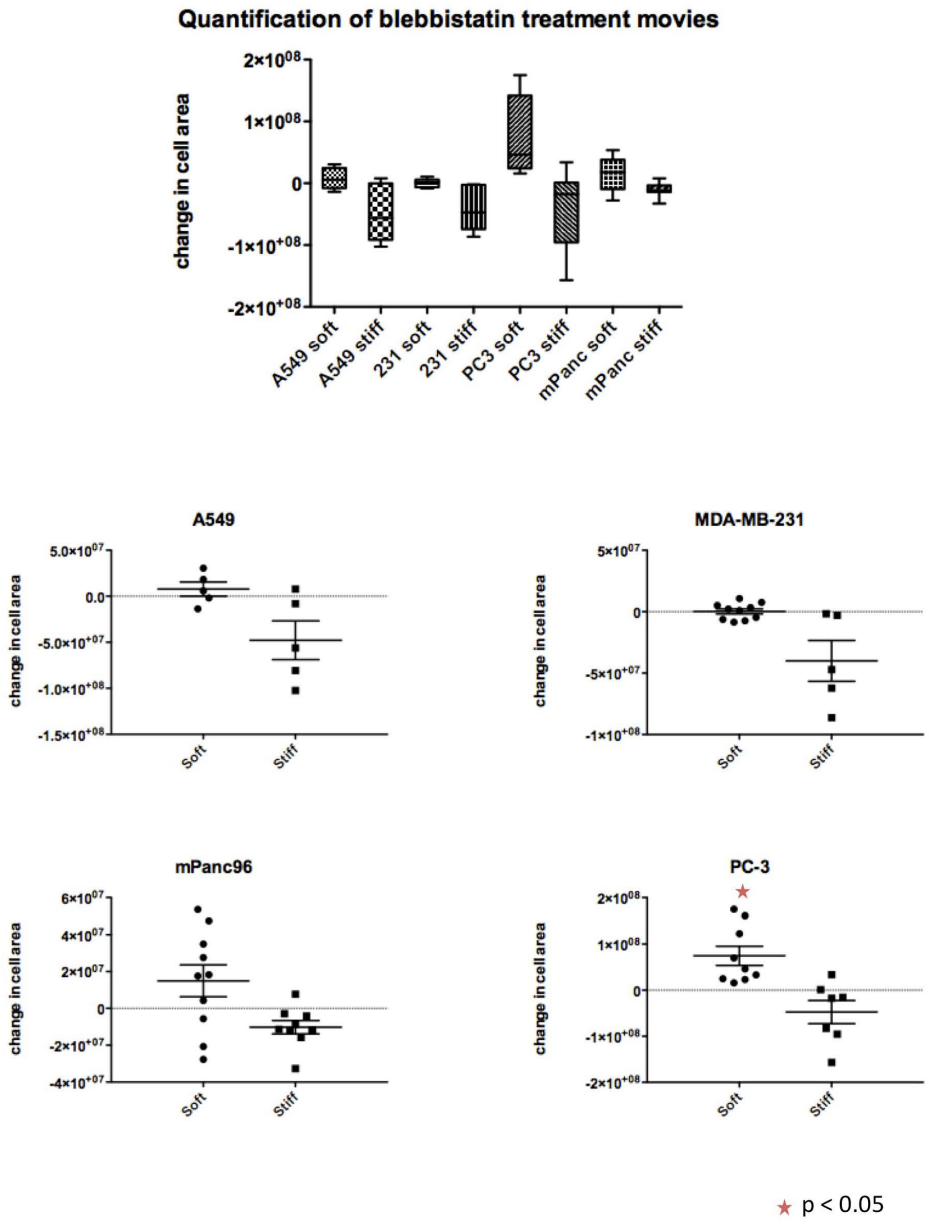
Quantification of blebbistatin treatment movies
change in cell area
2×10^08
1×10^08
0
-1×10^+08
-2×10^+08
A549 soft
A549 stiff
231 soft
231 stiff
PC3 soft
PC3 stiff
mPanc soft
mPanc stiff
A549
MDA-MB-231
mPanc96
PC-3
Soft
Stiff
★ p < 0.05

Discussion

This thesis presents preliminary investigations of the mechano-sensory mechanisms that enable some cancer cells to grow regardless of ECM rigidity. Examination of integrin expression demonstrated a correlation between increased α_2-integrin expression and rigidity-insensitivity, however the lack of a rigidity-specific response in the function blocking experiment suggests α_2 does not contribute to cell growth in a rigidity-specific manner. The contribution of myosin II to growth was assessed by inhibition on different rigidities. Myosin function was found to be critical for growth in all the cell lines on all the rigidities, supporting the conclusion that myosin II-driven tension is necessary even on soft substrates. While morphology changes due to 24hr myosin inhibition did not correlate with growth patterns, cell area changes after short-term treatment suggest differential tension states for rigidity-sensitive and rigidity-insensitive cells on soft substrates. However, the experiment does not exclude the possibility of differential actin polymerization dynamics. In addition to these observations, a correlation between increased myosin IIC expression and rigidity-insensitivity suggests this particular myosin isoform might play a role in the increased tension state of the rigidity-insensitive cell lines. Analysis of focal adhesion protein expression demonstrated a correlation between p130Cas upregulation and rigidity-insensitivity. Since p130Cas is a scaffolding protein, perhaps over-expression would lead to higher levels of signaling complex formation and increased downstream growth signals. Clearly defined focal adhesions were not visible on soft substrates, however optical limitations prevent

a conclusive argument for the absence of any type of adhesion on these substrates. Examination of protrusive behavior of the different cells on soft and stiff gels showed a common blebbing phenotype on soft gels, while on stiff gels there was a mix of blebbing and ruffling that did not correlate with growth patterns. Overall, these data argue that rigidity-insensitive growth correlates with multiple levels of dysregulation within focal adhesion proteins and myosin-driven contractility.

Integrins have long been known to be both mechano-tranducers as well as mechano-sensors, critical for generating adhesion growth signals (Friedland, Lee, Boettiger 2009; Puklin-Faucher and Sheetz 2009). Changes in tension can alter the affinity state and ligand interaction of integrins, forcing clustering of integrins converts normal cells to a malignant phenotype and function blocking β_1-integrins can revert cancer cells from a malignant phenotype (Orr and others 2006; Paszek and others 2005; Weaver and others 1997). Thus investigating the role collagen binding integrins play in the rigidity-sensitivity of cancer cell lines in the PA gel system was a logical first step. While the correlation between higher α_2-integrin expression and rigidity-insensitivity was compelling, blocking the function of α_2 with antibodies did not result in a rigidity-specific response. In fact, the PC-3 cells did not show any growth effect from the α_2-blocking antibody, perhaps due to the fact they also express α_1. The mPanc96 cells do not express α_1 and had significant decreases in growth due to α_2 blockade across all rigidities. The data indicate that whatever contribution α_2 has toward pro-growth signals, it is not sensitive to changes in rigidity.

Myosin II is the critical motor that drives tension generation through the actin cytoskeleton. The Rho-ROCK signaling pathway, amongst others, regulates myosin activity, and Rho-driven tension is known to be upregulated in cancer cells (Fritz, Just, Kaina 1999; Webb 2003). Recent work with glioma cell lines demonstrated that inhibiting myosin rescues migration of these cells on soft matrices (Ulrich, de Juan Pardo, Kumar 2009). Myosin inhibition in the four cancer cell lines tested resulted in growth suppression on all rigidities. Partial inhibition with 10μM blebbistatin lead to partial growth inhibition, but still the same rigidity-sensitivity of each cell line. This supports the conclusion that myosin-driven tension is critical for growth, even in cells on soft gels. While tension is generally thought to propagate along actin stress fibers anchored to mature focal adhesions, it is possible that cross-linking of the cortical actin network provides a framework on which myosin can generate tension in the absence of mature adhesions, as is the case in cells on soft gels. How this would affect signaling complexes generally associated with focal adhesions is unknown.

Cells adhered to the PA gel substrates can deform the flexible PA gels by pulling on them (Wang and Lin 2007). The different gels will deform more or less according to their rigidities. Likewise, a cell will deform a given gel more or less than another cell based on the amount of force applied through the adhesion - force that is generated by myosin. Thus the amount of myosin-driven tension in a cell can be expressed by how much a cell deforms a soft matrix. This is the basis for traction force microscopy. If the ability of the cells to pull on the gel is abolished with blebbistatin, the immediate response would be relaxation of gel

and cytoskeleton. The amount of relaxation would be related to the initial amount of force the cell was exerting on the gel. The relaxation of the gel and cytoskeleton would lead to a change in cell shape or area. If the assumption that change in cell area is related to the amount of force the cells were initially applying to the gel and thus the amount of tension the cell is under, then the PC-3 and mPanc96 cells were under more tension on the soft gels than the A549 or MDA-MB-231. It is important to differentiate between the immediate effects of blebbistatin on cell morphology versus potential long-term effects seen after extended treatment. As noted before the cell size and shape changes by 24hrs are inconsistent with growth patterns on either gel rigidity. It is not known what feedback signals could be influencing the cytoskeleton or adhesion formation in the different cell lines when blebbistatin is present for longer periods of time. Also, this experiment does not rule out the possibility that the immediate changes in cell area are influenced by actin polymerization, and it could be that actin dynamics are different in rigidity-insensitive cell lines. The possibility that rigidity-insensitive cells are under more tension correlates with the observation that myosin IIC expression is higher in those cells as well, although it is not clear how myosin IIC contributes to tension generation in addition to the other two isoforms in these cells.

Focal adhesions form anchors to the cell's substrate. In addition to integrins, the FA scaffolds talin and p130Cas have been shown to undergo conformational changes that promote complex formation in response to tension (del Rio and others 2009; Sawada and others 2006). FAK and Src, two kinases

responsible for propagating adhesion signaling, are described as mechano-responsive molecules (Vicente-Manzanares and others 2009). While focal adhesions were not visible on soft gels, optical limitations mean that structures such as nascent adhesions would not have been detectable. The alternative approach of looking at focal adhesion protein expression showed that p130Cas is present at higher levels in rigidity-insensitive cells. Perhaps increased p130Cas in cells which are under more tension promotes signaling downstream of Cas, such as to Rac.

Growth of cells on gels is known to influence protein expression (Chiquet and others 2009; Engler and others 2004). Mesenchymal stem cells respond to specific rigidities by differentiating into cell types that correspond with a particular rigidity, such as muscle or bone (Engler and others 2006). Previous work demonstrated the A549 cells upregulate expression of E-cadherin after 5 days of culture on soft gels, while E-cadherin is undetectable on stiff gels (Tilghman et al. manuscript submitted). Examination of p130Cas and MIIC expression after 5 day culture on soft or stiff gels indicate a trend of decreasing expression in PC-3, MDA-MD-231, and A549 cells. While the decrease in expression does not correlate with rigidity growth responses, it does raise the possibility of expression regulation of mechanosensory proteins by rigidity. Further work is needed to elucidate whether this is significant, occurs in more proteins, and what is responsible for the altered expression levels.

Characterization of cellular phenotype on soft and stiff gels demonstrated a common blebbing phenotype amongst all the cell lines on the soft gels.

Surprisingly, the A549 and mPanc96 cells showed mostly blebbing on stiff gels as well. The PC-3 and MDA-MB-231 cells spread and formed ruffling lamellipodia on the stiff gels. Blebbing is commonly associated with weak adhesion and soft substrates as well as activation of Rho, while protrusion and ruffling is associated with adhesion formation and Rac activity (Lammermann and Sixt 2009). This would suggest greater Rho activity and possibly increased MLC phosphorylation and contractility on the soft gels, while the mPanc96 and A549 blebbing on stiff gels disagrees with the conclusion that rigidity-insensitive cell lines generate more Rho-mediated tension. However, the data collected do not indicate the source of the blebbing phenotypes, so the inconsistencies would need to be resolved by higher resolution microscopy and quantitative analysis such as Rho and Rac activation assays.

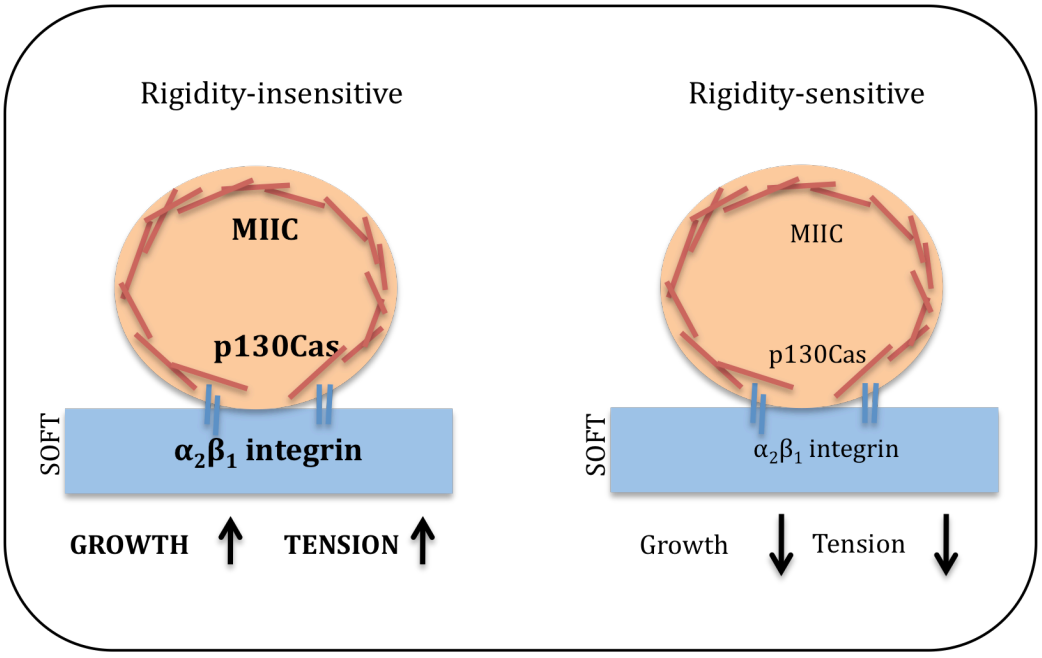

The data collected in this thesis provide evidence of mechano-sensory pathways altered in cancer cells that might help promote rigidity independent

growth. Upregulation of critical focal adhesion signaling components as well as tension generation machinery offer clues as to how some cancer cells continue proliferating in the absence of stiff ECM cues.

There are many questions that have been raised by this work, due largely in part to the preliminary nature of the data. Further experiments using knockdown and over-expression of α_2 integrin to mimic the differences in the cell lines will help to firmly establish its role in growth signal generation. Traction force microscopy can be used to directly address the question of how much force each cell type actually generates on a particular rigidity gel. Likewise, examination of not only protein expression level but activation states (by site specific phosphorylation Western blotting, for example) is critical to understand the signals propagated by p130Cas, MIIC and other proteins. Changes in protein expression and activation due to rigidity must also be further explored since growth signal propagation in soft environments is what is truly important in driving rigidity-insensitive growth. Ultimately, a better understanding of how cancer cells drive rigidity-insensitive growth will provide targets for therapeutic inhibition in a clinical setting.

References

Assoian RK and Klein EA. 2008. Growth control by intracellular tension and extracellular stiffness. Trends Cell Biol 18(7):347-52.

Chiquet M, Gelman L, Lutz R, Maier S. 2009. From mechanotransduction to extracellular matrix gene expression in fibroblasts. Biochim Biophys Acta 1793(5):911-20.

Choi CK, Vicente-Manzanares M, Zareno J, Whitmore LA, Mogilner A, Horwitz AR. 2008. Actin and alpha-actinin orchestrate the assembly and maturation of nascent adhesions in a myosin II motor-independent manner. Nat Cell Biol 10(9):1039-50.

del Rio A, Perez-Jimenez R, Liu R, Roca-Cusachs P, Fernandez JM, Sheetz MP. 2009. Stretching single talin rod molecules activates vinculin binding. Science 323(5914):638-41.

Engler AJ, Sen S, Sweeney HL, Discher DE. 2006. Matrix elasticity directs stem cell lineage specification. Cell 126(4):677-89.

Engler AJ, Griffin MA, Sen S, Bonnemann CG, Sweeney HL, Discher DE. 2004. Myotubes differentiate optimally on substrates with tissue-like stiffness:

Pathological implications for soft or stiff microenvironments. J Cell Biol 166(6):877-87.

Friedland JC, Lee MH, Boettiger D. 2009. Mechanically activated integrin switch controls alpha5beta1 function. Science 323(5914):642-4.

Fritz G, Just I, Kaina B. 1999. Rho GTPases are over-expressed in human tumors. Int J Cancer 81(5):682-7.

Galbraith CG, Yamada KM, Sheetz MP. 2002. The relationship between force and focal complex development. J Cell Biol 159(4):695-705.

Huang S and Ingber DE. 2005. Cell tension, matrix mechanics, and cancer development. Cancer Cell 8(3):175-6.

Lammermann T and Sixt M. 2009. Mechanical modes of 'amoeboid' cell migration. Curr Opin Cell Biol 21(5):636-44.

Levental KR, Yu H, Kass L, Lakins JN, Egeblad M, Erler JT, Fong SF, Csiszar K, Giaccia A, Weninger W, et al. 2009. Matrix crosslinking forces tumor progression by enhancing integrin signaling. Cell 139(5):891-906.

Liu Z, van Grunsven LA, Van Rossen E, Schroyen B, Timmermans JP, Geerts A, Reynaert H. 2010. Blebbistatin inhibits contraction and accelerates migration in mouse hepatic stellate cells. Br J Pharmacol 159(2):304-15.

Lo CM, Wang HB, Dembo M, Wang YL. 2000. Cell movement is guided by the rigidity of the substrate. Biophys J 79(1):144-52.

Orr AW, Ginsberg MH, Shattil SJ, Deckmyn H, Schwartz MA. 2006. Matrix-specific suppression of integrin activation in shear stress signaling. Mol Biol Cell 17(11):4686-97.

Paszek MJ, Zahir N, Johnson KR, Lakins JN, Rozenberg GI, Gefen A, Reinhart-King CA, Margulies SS, Dembo M, Boettiger D, et al. 2005. Tensional homeostasis and the malignant phenotype. Cancer Cell 8(3):241-54.

Pelham RJ,Jr and Wang Y. 1997. Cell locomotion and focal adhesions are regulated by substrate flexibility. Proc Natl Acad Sci U S A 94(25):13661-5.

Provenzano PP, Inman DR, Eliceiri KW, Keely PJ. 2009. Matrix density-induced mechanoregulation of breast cell phenotype, signaling and gene expression through a FAK-ERK linkage. Oncogene 28(49):4326-43.

Puklin-Faucher E and Sheetz MP. 2009. The mechanical integrin cycle. J Cell Sci 122(Pt 2):179-86.

Sawada Y, Tamada M, Dubin-Thaler BJ, Cherniavskaya O, Sakai R, Tanaka S, Sheetz MP. 2006. Force sensing by mechanical extension of the src family kinase substrate p130Cas. Cell 127(5):1015-26.

Somlyo AP and Somlyo AV. 2003. Ca2+ sensitivity of smooth muscle and nonmuscle myosin II: Modulated by G proteins, kinases, and myosin phosphatase. Physiol Rev 83(4):1325-58.

Tzima E, del Pozo MA, Shattil SJ, Chien S, Schwartz MA. 2001. Activation of integrins in endothelial cells by fluid shear stress mediates rho-dependent cytoskeletal alignment. EMBO J 20(17):4639-47.

Ulrich TA, de Juan Pardo EM, Kumar S. 2009. The mechanical rigidity of the extracellular matrix regulates the structure, motility, and proliferation of glioma cells. Cancer Res 69(10):4167-74.

Vicente-Manzanares M, Ma X, Adelstein RS, Horwitz AR. 2009. Non-muscle myosin II takes centre stage in cell adhesion and migration. Nat Rev Mol Cell Biol 10(11):778-90.

Wang F, Weaver VM, Petersen OW, Larabell CA, Dedhar S, Briand P, Lupu R, Bissell MJ. 1998. Reciprocal interactions between beta1-integrin and epidermal growth factor receptor in three-dimensional basement membrane breast cultures: A different perspective in epithelial biology. Proc Natl Acad Sci U S A 95(25):14821-6.

Wang HB, Dembo M, Wang YL. 2000. Substrate flexibility regulates growth and apoptosis of normal but not transformed cells. Am J Physiol Cell Physiol 279(5):C1345-50.

Wang JH and Lin JS. 2007. Cell traction force and measurement methods. Biomech Model Mechanobiol 6(6):361-71.

Wang YL and Pelham RJ,Jr. 1998. Preparation of a flexible, porous polyacrylamide substrate for mechanical studies of cultured cells. Methods Enzymol 298:489-96.

Weaver VM, Petersen OW, Wang F, Larabell CA, Briand P, Damsky C, Bissell MJ. 1997. Reversion of the malignant phenotype of human breast cells in three-dimensional culture and in vivo by integrin blocking antibodies. J Cell Biol 137(1):231-45.

Webb RC. 2003. Smooth muscle contraction and relaxation. Adv Physiol Educ 27(1-4):201-6.

Wozniak MA, Desai R, Solski PA, Der CJ, Keely PJ. 2003. ROCK-generated contractility regulates breast epithelial cell differentiation in response to the physical properties of a three-dimensional collagen matrix. J Cell Biol 163(3):583-95.

Yeung T, Georges PC, Flanagan LA, Marg B, Ortiz M, Funaki M, Zahir N, Ming W, Weaver V, Janmey PA. 2005. Effects of substrate stiffness on cell morphology, cytoskeletal structure, and adhesion. Cell Motil Cytoskeleton 60(1):24-34.